ACKNOWLEDGEMENTS

The author expresses his gratitude to his report supervisor, Dr. S. Sankar, for his valuable guidance and encouragement, and the help extended during the preparation of this report. I would also like to thank Miss Velia Durestante for her help in translation and also Mrs. Julie Strick for the typing this report.

Montreal, Quebec
October 1977

A. Razavizadeh

TABLE OF CONTENTS

NOMENCLATURE

a - Distance between vehicle C.G. and front wheel center, (Figs. 2.1 and 3.1), ft.

a_1 - Location of the sprung mass C.G. in X"Y"Z". Frame measured from point 1 (Fig. 3.9) ft.

A - Wheel 1 and ground contact point, origin of X'Y'Z' frame.

A_f - Largest car sectional area, ft^2.

A' - Empirical number A' = 12.5/1000, ft/sec.

b - Distance between vehicle C.G. and rear wheel centre (Figs. 2.1 and 3.1), ft.

b_1 - Location of the sprung mass C.G. in X"Y"Z" - frame measured from point 1 (Fig. 3.9), ft.

$B_{1,2}$ - Rolling moment on the unsprung masses about the roll axes of the unsprung mass, front and rear, respectively, lb. ft.

c - X-coordinate of C.G. of the unsprung mass (Fig. 3.1), ft.

C_1 - Location of the sprung mass C.G. in X"Y"Z" - frame measured from point 1 (Fig. 3.9), ft.

C_{ij} - Tire cornering stiffness $\left\{ \left(= \frac{\partial F_{ij}}{\partial \alpha_{ij}} \right)_{\substack{\alpha_{ij}=0 \\ \Theta_{ij}=0}} \right\}$ lb.

$C_{c_{ij}}$ - Tire camber thrust stiffness $\left\{\left(= \frac{\partial F_{ij}}{\partial \alpha_{ij}}\right)_{\substack{\alpha_{ij}=0 \\ \theta_{ij}=0}}\right\}$ lb.

C_s - Shock absorber damping constant, lb_f-sec/ft.

C_t - Tire damping constant, lb_f-sec/ft.

$C_{\zeta\xi}$ - Product of inertia of the sprung mass about the η_s-axis, slug - ft^2

d_s - Maximum safe deceleration.

e - Deistance between the C.G. of the sprung mass and the main roll axis (= h cos λ + c Sin λ) (Fig. 3.1), ft.

e' - Location of the wind load below the centroid of the sprung mass, ft.

f - Tire road adhesion coefficient.

F_{ij} - Horizontal side force on tire (due to tire slip and camber angles) acting perpendicular to the intersection of the road and the plane of symmetry of the wheel (Fig. 3.2), lb.

F_{vij} - Total vertical load (static and dynamic load), lb_f.

g - Acceleration due to gravity 32.2, ft/sec.^{2}.

h - Height of the C.G. of the sprung mass above the ξ_s axis (Fig. 3.1), ft.

h_m - Height of the C.G. of the entire vehicle above the road (Fig. 3.1), ft.

h_w - Equilibrium height of wheel when the car is at rest, ft.

H - Moment of momentum, lb_f-ft-sec.

I - Moment of inertial of the sprung mass, lb_f-ft-sec.^{2}

I_{XZ} - Product of inertia of the vehicle about an axis parallel to the Y-axis but passing through the Z-axis at road height, slug-ft.^{2}

$I_{\zeta s}$ - Polar moment of inertia of the sprung mass about the ζ_s-axis, slug-ft^2.

$I_{\eta s}$ - Polar moment of inertia of the sprung mass about the η_s-axis, slug-ft^2.

$k_{1,2}(\phi-\phi_{1,2})$ - Rolling moment on sprung mass about the roll centres of the sprung mass, front and rear respectively, lb-ft.

k_s - Steel spring constant, lb_f/ft.

K_t - Tire spring constant (appropriate British units).

$\mathcal{L}$ - Wheel base (distance between front and rear wheel axles), ft.

ℓ_s - Equilibrium length of the steel spring when the car is at rest, ft.

L - Lateral tire forces, lb.

M - Total mass of vehicle, slugs.

M_s - Mass of sprung body, slugs.

M_u - Total unsprung mass, slugs.

$M_{1,2}$ - Unsprung mass, front and rear, respectively, slugs.

N - Total aligning moment, lb-ft.

N_t - Total moment about the Z-axis, due to tire force, lb-ft.

N_{ij} - Aligning torque on a tire, about a vertical axis, lb-ft.

$N_{ijX'}$ - Moment about the sprung mass C.G. in X'-direction by the lateral forces on the 4 tires, lb-ft.

$N_{ijY'}$ - Moment about the sprung mass C.G. in Y'-direction by the longitudinal forces on the 4 tires, lb-ft.

n_y - Lateral acceleration of the C.G. of the vehicle, away from the turn centre, ft/sec^2.

O - Origin of the inertia frame, XYZ.

P_{th} - Total driving thrust, lb.

P_{ij} - Driving thrust on an individual wheel, lb.

r - Wheel radius (axle to road), ft.

1/R - Path curvature, 1/ft.

S - Braking tire forces lb_f.

x

$S_{1,2}$ - Braking force on the front and rear wheel respectively, lb_f.

S_α - Aerodynamic force; lb_f.

S_{Hij} - Summation of horizontal forces on a tire, lb.

S_i - Inertia force, lb_f.

S_{ij} - Longitudinal force on each tire in X'-direction, lb_f.

S_{ijs} - Longitudinal force on the sprung mass in X'-direction, lb_f.

$t_{1,2}$ - Front and rear axle tread, respectively, ft.

T - Driveshaft torque, lb-ft.

v - Lateral velocity of vehicle along Y axis, ft/sec.

v_{ij} - Resultant velocity at the centre of the contact region of each tire, ft/sec.

V - Forward velocity of vehicle, ft/sec.

W - Total weight of vehicle, lb.

W_{ij} - Longitudinal force on a tire, parallel to the wheel plane, lb.

W_s - Sprung weight, lb.

W_u - Total unsprung weight, lb.

$W_{u_{1,2}}$ - Front and rear unsprung weight, respectively, lb.

$\dot{x}$ - Absolute velocity of the reference point O in the x-axis, ft/sec.

X_w - Wind force, lb.

X_{ij} - Total force in the X-axis, front and rear, respectively, lb_f.

X Y Z - Inertia frame origin at O.

X'Y'Z' - Frame origin at A, moving with the car, X' axis passing through right front wheel, and Y' axis passing through left rear wheel.

X"Y"Z" - Frame origin at 1, fixed in the sprung mass.

$X"_c Y"_c Z"_c$ - Frame origin at C.G. (the centroid of the sprung mass) $X"_c X"$, $Y"_c Y"$, $Z"_c Z"$.

X_i, Y_i - Location of the i^{th} wheel in inertial frame, ft.

$\dot{X}_i, \dot{Y}_i$ - Velocity of the i^{th} wheel in inertia frame, lb/sec.

$\ddot{X}_i, \ddot{Y}_i$ - Acceleration of the i^{th} wheel in inertia frame, ft/sec^2.

X'_i, Y'_i - Location of the i^{th} wheel in terms of i'j'k', ft.

$\dot{X}'_i, \dot{Y}'_i$ - Velocity of the i^{th} wheel in terms of i'j'k', ft/sec.

$\ddot{X}'_i, \ddot{Y}'_i$ - Acceleration of the i^{th} wheel in terms of i'j'k', ft/sec^2.

$\dot{y}$ - Absolute velocity of the reference point O in the Y direction, ft/sec.

Y_{ij} - Force in the Y direction on an individual tire, lb.

$Y_{1\&2}$ - Total tire force in the Y-direction, front and rear, respectively, lb.

$Z_{1,2}$ - Negative Z-coordinate of the sprung-mass roll centres, front and rear, respectively, (Fig. 3.1), ft.

Z_{ij} - Vertical load on an individual wheel, lb.

Z_{ij_2} - Tire deflections (functionof time) from their individual equilibrium positions, i.e. measured in the inertia frame, ft.

Z_{ij_3} - Spring and shock absorber deflections (function of time) from their individual equilibrium positions, i.e. measured in the inertia frame, ft.

α_{ij} - Slip angle at an individual tire (Fig. 3.2).

β - Vehicle side slip angle.

β_{ij} - Sideslip angle of the contact centre of an individual tire, Fig. 3.2.

γ_{ij} - Angle between wheel centre-plane and the x-axis of the vehicle (Fig. 3.2).

δ_{ij} - Input steer angle (equal to zero for the rear wheels), Fig. 3.2.

δ - Average input steer angle.

θ_{ij} - Camber angle of individual wheel.

ρ - Air density, slugs/ft^2.

ρ - $\rho = a_1 i'' + b_1 j'' + c_1 k''$

ψ - Yawing velocity of the vehicle, 1/sec or deg/sec.

ϕ - Roll angle of the sprung mass about the unsprung roll axis, rad.

$\phi_{1,2}$ Roll angle of the unsprung mass about the unsprung roll axis, front and rear, respectively.

θ - Pitch angle, vector in the Y'-direction, rad.

λ - Angle between the x-axis and the roll axis of the unsprung mass (Fig. 3.1).

ξ_s, η_s, ζ_s - Axes fixed in the sprung mass; the origin Ω, lies on the sprung-mass roll axis, the ξ_s-axis is parallel to the sprung-mass roll axis and lies in the plane of symmetry of the vehicle when at rest, the ζ_s-axis passes through the c.g. of the entire vehicle and lies in the plane of symmetry and the η_s-axis is perpendicular to the ξ_s, ζ_s plane.

n - Gear ratio of differential (final drive ratio).

χ_{ij} - Wheel toe angle (Fig. 3.2).

Indices

1	Front	i
2	Rear	i
L	Left	j
R	Right	j
s	Sprung	
u	Unsprung	
W	Due to wind	
ζ	About the ζ_s-axis	
η	About the η_s axis	
ξ	About the ξ_s axis	

LIST OF FIGURES

LIST OF TABLES

CHAPTER 1

INTRODUCTION

1.1 GENERAL

When a car is moving it possesses kinetic energy that has to be lost before it can stop. If the engine ceases to drive the car, this energy could be lost in overcoming air resistance and by turning the engine and transmission against friction. This process of stopping a moving car, however, would take some time to happen, so brakes are fitted to decelerate the car by converting the kinetic energy into heat which could be lost to the surrounding air. As a considerable quantity of heat may be involved, the brakes must be able to lose the generated heat easily and rapidly. Therefore, brakes must be designed in such a way that temperatures do not exceed the safe critical limit. Since the kinetic energy of a moving car is dependent on the weight of the car and its speed squared, heavy and fast cars should have better brakes, than those which are essentially light and slow. Thus, the brakes used on heavier cars are often designed to lose a larger amount of heat more rapidly.

1.2 TYPES OF BRAKES IN VEHICLES

Brakes commonly used on road vehicles may be identified as one of the following basic types:

1.2.1 Drum Brake Type [1]

Drum brakes are still widely used and are invariably expanding brakes in which the brake shoes are brought into contact with the inside of the brake drum by means of an expanding mechanism.

The principle of the internal expanding rigid-shoe brake is shown in Fig. 1.1. The brake drum A is fixed to the hub of the road wheel (shown in chain dotted lines) by bolts which pass through its flange. The inner side of the drum is open, and a pin B projects into it. This pin is carried in an arm C which is either integral with, or secured to, the axle casing. The brake shoes D and E are free to pivot on the pin B. They are roughly semicircular, and in between their lower ends is a cam M. The latter is integral with, or is fixed to, a spindle N, free to turn in the arm Q of the axle casing. A lever P is fixed to the end of the cam spindle, and when this lever is pulled by a rod which is coupled to its end, the cam spindle and cam are turned round slightly, thus moving the ends of the brake shoes apart. The shoes are thus pressed against the inside of the brake drum, and frictional forces act between them, tending to prevent any relative motion. The frictional force thus tends to slow down the drum, but it also tends to make the shoes revolve with the drum. The latter action is prevented by the pin B, and the cam M. The pin B is therefore called the "anchorage" pin.

1.2.2 Disc brake type [1]

The simplest construction of disc brake is the Fixed Calliper Double Piston Type, as shown in Fig. 1.2. The disc A is secured to the wheel hub which rotates on bearings on the axle casing or stub axle, depending on whether a rear or a front brake is concerned. A calliper

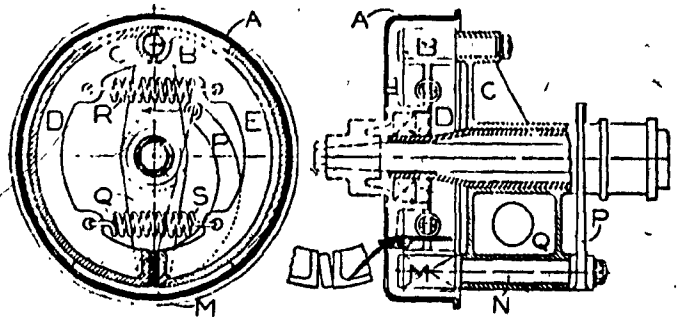

Fig. 1.1 - Shoe Brake Type (Ref. 1)

member C is bolted to the member B, which will be referred to as the mounting. Two pistons D and E are positioned inside the cylinder formed in the calliper. These house two pads consisting of a metal plate to which friction material facing are bonded. The metal plates fit in the recesses of the calliper so that they are prevented from rotating with the disc. The callipers of such brakes usually have to be made in two parts to enable the cylinders to be machined and also must have openings through which the friction pads can be removed for replacement.

The advantages of the disc brakes are:

1. The area of the pads are smaller as compared with the area of lining for drum type. Therefore, the temperature rise is smaller and consequently the pads are less subjected to wear and hence their life is comparable with that of a drum brake.

2. The action of the disc brake is unaffected by the occurrence of wear or by expansion due to rise in temperature, both of which are sources of trouble in drum brake.

Both types of brakes may be operated mechanically or hydraulically, either by hand or foot. They may be operated by the driver manually or with power assistance. In general, all modern cars use a similar layout for the brakes. When the brake is applied, torque has to be transmitted from the tire to axle through the drum or disc which is fixed to the wheel. It is also necessary to anchor the brake linings so that they cannot rotate, and for this reason some form of torque arm is used.

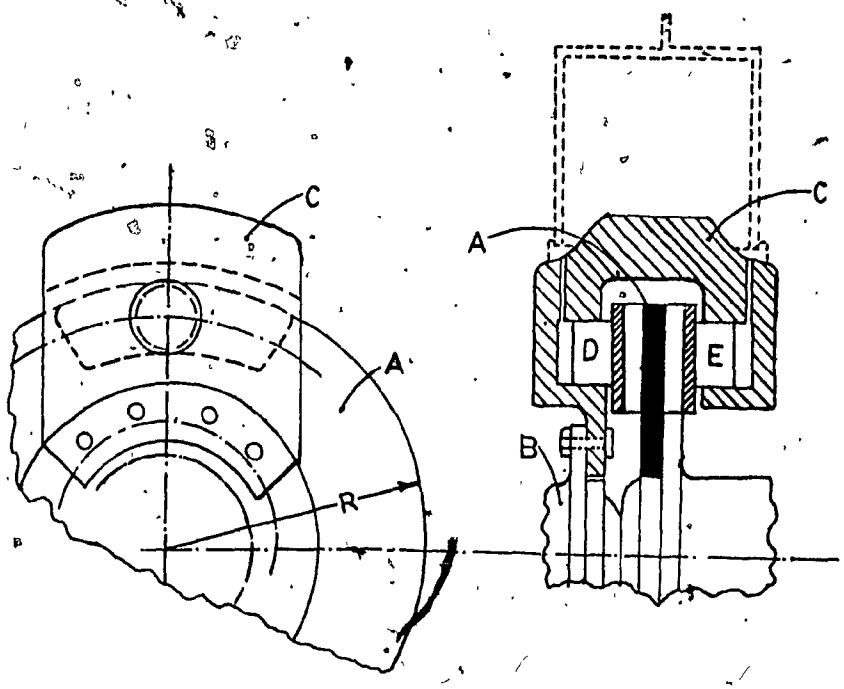

Fig. 1.2 - Disc Brake Type

1.3 Vehicle Deceleration Phenomenon

The maximum deceleration which can be achieved on a road vehicle is generally associated with the coefficient of friction between the tire and the road surface. The safe limit of deceleration during braking can be said to occur when one wheel locks, since directional control may then be lost. While braking, the load distribution varies due to cornering and deceleration-force and to changes in static loading. If the braking distribution is identical to the instantaneous load distribution, then the maximum value of safe limit can be achieved. Hence, a variable braking distribution is required if this ideal performance is to be approached. Emergency conditions involving heavy braking or accelerating, or sudden manoeuvres are not well described by steady state solution or linearized system of forces. To deal completely with vehicle behaviour under such conditions, transient type solution must be found.

1.4 Discussion on Earlier Works on Vehicle Dynamics During Braking

Adhesion utilization defined as the ratio of the deceleration obtainable without wheel locking to the deceleration with wheel locked has an important role on deceleration of a car without loss of steering control due to wheel locking. This ratio has been calculated for variety of road surfaces. Troost [2] and Strein [3] have developed the method of "adhesion utilization", which is the ratio of d/f where d = maximum safe deceleration and f = tire-road adhesion coefficient. If d/f = 1.0, the braking distribution is called to be ideal. Rouse [4] has calculated the value of coefficient of adhesion and suggested a number of ways of alter-

ing the braking ratio. Similarly, Dunlop [5] used the deceleration of the vehicle in order to control the braking ratio directly. He suggested that all classes of vehicles should be capable of using to the full the maximum tire-road adhesion which is available, since poor road surfaces are bound to exist, if only temporarily.

Skidding forms the subject of a paper by Jones [6] which describes various phenomena experienced during sudden braking. Radt and Milliken [7] developed expressions for the performance of a tire when adhesion is completely lost. These expressions were then used to compute the performance of a hypothetical vehicle which has a steady forward speed under the action of considerable fore and aft forces.

The Clayton Dewandre control valve [8] for commercial vehicles similarly controls the braking ratio by making the deflection of axle suspension under load, shift the fulcrum of the balance beam connecting the two pistons.

The equation of motion of a car, using body centred axes, are developed by Duncan [9]. He also provided a critical discussion on the importance of the stability criterion. Many of the stability and control of aircrafts, discussed by Duncan is also applicable to vehicle analysis. One of the major contributions to the study of vehicle dynamics is the series of paper by the staff of the Cornell Aeronautical Laboratory [10]. In these papers the equations of motion are developed using a body centred axis system. Constant forward speed is assumed, and the side slip angles of the tires are limited to some 5^{o} so that a linear relation is obtained between sideslip angle of the tire and the lateral force developed. The tire forces are also considered and is assumed to be ineffective to the

demands of thrust for accelerating or braking. By considering the combined effect of load transfer and power transmission through the driven wheels, Eillis [11] suggests a method whereby the handling responses may take account of the inter-axle roll stiffness distribution.

Rocard [12] describes the motions of a non-rolling vehicle using earth reference axes. Since the equations of motion are in the (x, y, e) axes, this analysis forms an excellent introduction to the subject of vehicle control.

Saible and Shang [13] investigated on the dynamics of an automobile in braking and acceleration. They provided the transient response of an automobile involving sudden braking or acceleration in rectilinear motion. In order to deal with emergency conditions involving heavy braking, acceleration, or sudden manoeuvres, transient type vehicle analysis is essential. The study of vehicle dynamics in the references discussed above do not consider the vertical motion of the car, unequal brake action or the use of a four wheel model. In 1961, Saibel, Fox and Bergman [14] proposed a model for vehicles in the cornering manoeuver both on and off the highway. Saibel and Taso [15, 16] in 1968 extended this model for vehicles under sudden manoeuvers. In 1969 Tsao [17] included empirical relations to solve the above mentioned problem. Empirical equations, however, limit the practical application of this model. Saibel and Shang [13] did extensive research work on four-wheel automobiles as well as introducing and expanding on the non-linear tire characteristics. They also investigated the transient response of an automobile when the driver suddenly has locked wheels. The effect of road pattern, non-linear characteristics of tires, springs, dampers, and braking characteristics are also studied. They have shown that the magnitude of the braking force is much higher

than the rolling resistance and wind force, and hence they will have a minor effect on the analytical solution.

CHAPTER 2

VEHICLE BRAKING FORCE DISTRIBUTION ON ROADS

2.1 GENERAL

It is extremely important that all vehicles should be capable of the greatest possible deceleration without any loss of steering control due to wheels locking. To find out how much deceleration can be achieved, the 'adhesion utilization', defined as the ratio of the deceleration obtainable without wheel locking to the deceleration with wheels locked, has been calculated for a variety of road surfaces [2, 3].

The maximum deceleration which can be achieved on a road vehicle is generally associated with the coefficient of friction between the tire and the road surface. In general, the criterion of 'all wheels locked' on a good road surface is available as a measure of stopping power, and hence the effects of the distribution of braking between the wheels might be ignored. The safe limit of deceleration during braking can be said to occur when one wheel locks, since directional control may then be lost. Any measure which raises the level of deceleration before skidding occurs will make an overall contribution to general safety.

In the past, a fixed braking ratio between the axles has been used, since this is the simplest way of distributing the brake force. This practice has the advantage of simplicity and cheapness. With a fixed braking ratio, the minimum size of brakes can be used in obtaining the required

brake torque and dissipation of kinetic energy while giving uniformity of brake lining life.

One danger arising from the use of the simple fixed ratio braking systems is the variation of brake sensitivity which may be experienced. Passenger car drivers are familiar with the changes of pedal effort* that are required to combat either changes in the frictional properties of the brake or changes in vehicle weight due to the carrying of additional passengers.

Braking efficiency can be greatly improved by more realistic proportioning of the braking effort between the front and rear wheels of a vehicle. The proportioning should be set according to the load on those wheels under the influence of load transfer. This chapter describes how the braking forces are distributed on vehicle wheels.

2.2 External Forces Acting on a Car During Braking

In Fig. 2.1 all the external forces on a saloon car during braking are shown. Point E is the centre through which the air resistance acts; G is the centre of gravity, S_1 and S_2 are the braking forces on the front and rear wheels respectively, S_i is the inertia force, S_a is the aerodynamic force and F_{V1} and F_{V2} are the vertical forces on the front and rear wheels respectively. W indicates the weight of the vehicle.

For a state of equilibrium, the following set of equations for forces and moments can be written as [18]:

---

*Pedal effort is defined as the force that must be exerted on the brake pedal in order to produce the maximum deceleration permitted by the state of the road.

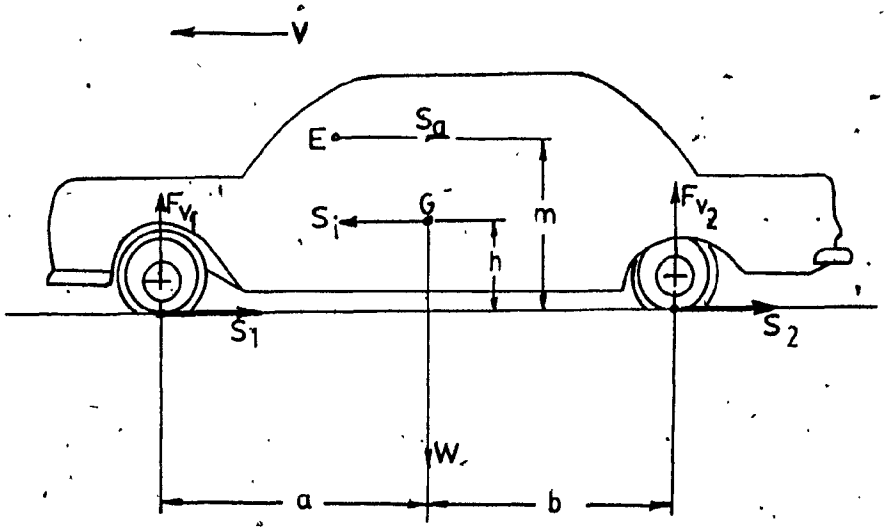

Fig. 2.1 - Illustration of External Forces on A Car During Braking

$$S_1 + S_2 + S_a = S_i \quad \ldots\ldots\ldots\ldots \quad (2.1)$$

$$F_{V1} + F_{V2} = W \quad \ldots\ldots\ldots\ldots\ldots\ldots \quad (2.2)$$

$$F_{V1}(a+b) + S_a m = S_i h + Wb \quad \ldots\ldots\ldots\ldots \quad (2.3)$$

where a, b, m and h are distances referred to in Fig. 2.1

If μ_{A_1} and μ_{A_2} are the coefficients of adhesion assumed for the front and rear wheel respectively, then

$$S_1 = \mu_{A_1} F_{V1} \quad \ldots\ldots\ldots\ldots\ldots\ldots \quad (2.4)$$

$$S_2 = \mu_{A_2} F_{V2} \quad \ldots\ldots\ldots\ldots\ldots\ldots \quad (2.5)$$

If the total braking moments on the front and rear wheels are N_1 and N_2 respectively, and since they are proportional to the pressure p of the braking fluid.

$$N_1 = k_1 p \quad \ldots\ldots\ldots\ldots\ldots\ldots \quad (2.6)$$

$$N_2 = k_2 p \quad \ldots\ldots\ldots\ldots\ldots\ldots \quad (2.7)$$

where k_1 and k_2 are the dimensional constants depending upon the arrangements and dimension of the brake shoes and the diameters of the brake drums or the equivalent characteristics in the case of disc brakes. Also

$$N_1 = S_1 R \quad \ldots\ldots\ldots\ldots\ldots\ldots \quad (2.8)$$

$$N_2 = S_2 R \quad \ldots\ldots\ldots\ldots\ldots\ldots \quad (2.9)$$

where R is rolling radius of tires.

The above set of equation can be rearranged and can be expressed under the assumption $S_a = 0$ as follows:

$$F_{V1} = W \frac{b + \mu_{A_2} h}{a+b+h(\mu_{A_2} - \mu_{A_1})} \quad \ldots\ldots\ldots\ldots\ldots \quad (2.10)$$

$$F_{V2} = W \frac{a - \mu_{A_2} h}{a+b+h(\mu_{A_2} - \mu_{A_1})} \quad \ldots\ldots\ldots\ldots\ldots\ldots \quad (2.11)$$

$$k_1 p = W \frac{b + \mu_{A_2} h}{a+b+h(\mu_{A_2} - \mu_{A_1})} \mu_{A_2} R \quad \ldots\ldots\ldots\ldots \quad (2.12)$$

$$k_2 p = W \frac{a - \mu_{A_1} h}{a+b+h(\mu_{A_2} - \mu_{A_1})} \mu_{A_2} R \quad \ldots\ldots\ldots\ldots \quad (2.13)$$

If p is eliminated from equations (2.12) and (2.13), then

$$\mu_{A_1} = ak \frac{\mu_{A_2}}{k_2 b + \mu_{A_2} h(k_1 + k_2)} \quad \ldots\ldots\ldots\ldots\ldots\ldots \quad (2.14)$$

Now the total braking moment and force on the wheels are given by

$$N_{total} = (k_1 + k_2)p = WR \frac{b\mu_{A_2} + a\mu_{A_2}}{a+b+h(\mu_{A_2} - \mu_{A_1})} \quad \ldots\ldots\ldots \quad (2.15)$$

where $N_{total} = N_1 + N_2$

and

$$S_{total} = \frac{N_{total}}{R} = (k_1 + k_2)p/R = W \frac{b\mu_{A_2} + a\mu_{A_1}}{a+b+h(\mu_{A_2} - \mu_{A_1})} \quad \ldots \quad (2.16)$$

Hence, using the expression for total braking force, the deceleration obtained under the condition that the wheels do not lock, can be expressed by —

$$d = S_{total} \frac{g}{W} = \frac{(k_1 + k_2)p}{WR} g = g \frac{b\mu_{A_1} + a\mu_{A_2}}{a+b+h(\mu_{A_2} - \mu_{A_1})} \quad \ldots\ldots \quad (2.17)$$

2.3 Road - Tire Adhesion

Adhesion properties of pneumatic tires on road has been studied earlier [19]. The adhesion like the friction between two surfaces, can be characterized by a coefficient called the coefficient of adhesion μ_A,

which is the ratio of the tangential force transmitted by the wheel to the normal load carried by the wheel. The term 'adhesion' is often used loosely when coefficient of adhesion is implied. The coefficient of adhestion is, in effect, the coefficient of friction.

The coefficient of adhesion, μ_A depends upon the material of the tire and its tread pattern, the material and texture of the road surfaces and the nature and thickness of any film present (water, mud, oil, etc.). For a typical rubber tire the coefficient of adhesion μ_A also depends upon sliding velocity and operating temperature [20]. Figs. 2.2 and 2.3 illustrate these facts. From Fig. 2.2 it can be seen that μ_A increases with the sliding velocity until a critical velocity. Once the sliding velocity is greater than that corresponding to the peak (critical velocity), any increase in sliding velocity, will decrease the frictional torque at the road surface. In this arrangement the wheel becomes unstable and locks. Fig. 2.3 indicates that a small amount of slip, called "creep" superimposed on the rotational velocity enables more torque to be handled. Some drivers utilize the peak adhesion by 'pumping' the brakes. The driver applies the brake several times a second releasing it just before the wheel is about to lock. It has been shown experimentally [14] that the stopping distance with pumping is less than with locked wheels on a wet surface. The antiskid devices also make use of the high adhesion available just before wheel locking occurs.

In general, μ_A decreases with increasing tire temperature; consequently once a tire skids, frictional heating over the small contact area on the tire causes the adhesion to fall still further. The temperature can be sufficient to melt the rubber or the binder on the road, forming the characteristic black skid marks. Tires of vehicles

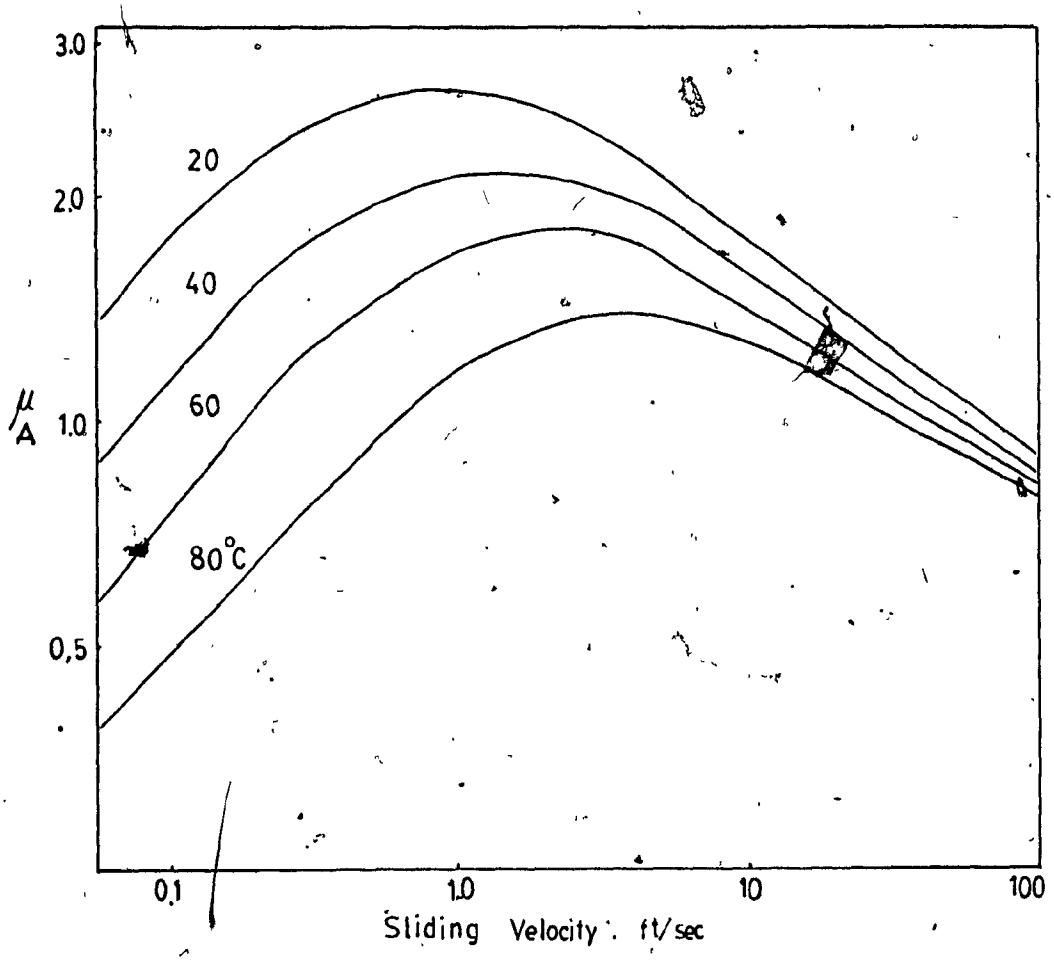

Fig. 2.2 - The Variation of the μ_A with Velocity of a Rubber at Various Temperatures (Log-Log Plot)

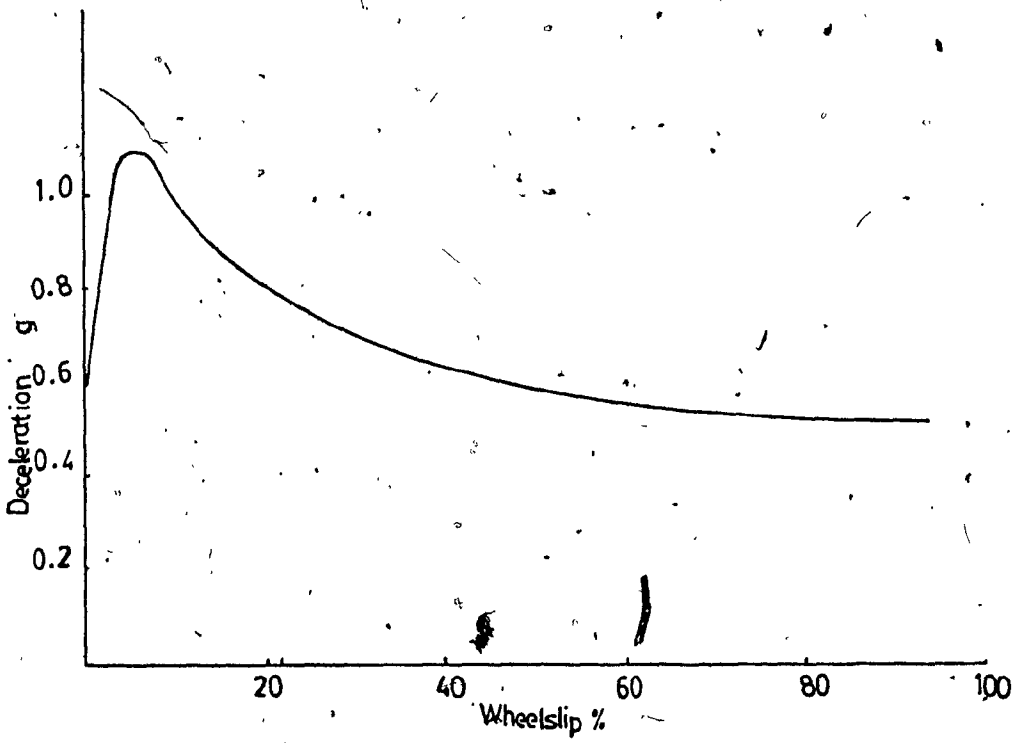

Fig. 2.3 - Typical Curve Showing How Deceleration Varies with Percentage of Wheel Slip

travelling at high speed can reach a temperature sufficient to lower the adhesion.

2.4 Directional Stability [21]

When a wheel is locked the direction of the frictional force is independent of the wheel orientation and hence the direction of the vehicle cannot be controlled. Consider the situation that the rear wheels are locked and that the vehicle is moving in a straight line as shown in Fig. 2.4. The centre of gravity (C.G.) of the vehicle will continue to move in the original direction, but if for some reason a small couple operates about a vertical line through the C.G., caused, for example, by uneven braking on the two sides of the vehicle, or by the road camber, the vehicle acquires an angular velocity $\omega = \frac{V}{R}$ about an instantaneous center O where V is its initial velocity and R is the distance between the instantaneous centre and the locked wheel. The centre O is at the intersection of the straight line through the front wheels and the straight line through the C.G. at right angles to the locus of the C.G. If the adhesion between road and tires is too small to balance the couple, the rear end of the vehicle will begin to swing around. But as the longitudinal axis of the vehicle deviates further from the locus of the C.G., the R decreases. Since the angular momentum has to be conserved, the angular velocity ω increases (v is considered to remain constant during the small time the skid develops) until the axis of the car is perpendicular to the direction of motion. Then ω begins to diminish until eventually it becomes zero and the vehicle proceeds stably with the rear wheels leading. The trajectory of the instantaneous centre of rotation is approximately a cusped tractrix.

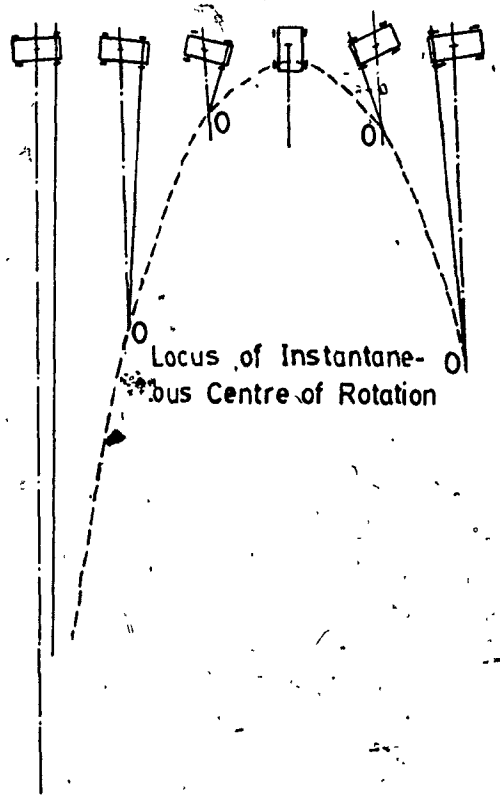

Fig. 2.4 - Illustration of Vehicle Movement When Rear Wheel Are Locked

If all four wheels lock simultaneously, the vehicle will slide down the camber out of control. If the rear wheels lock less than 0.5 sec. before the front wheels, the vehicle will continue to move ahead in a straight line. However, if one rear wheel locks before the other, no deviation occurs until both lock.

To get out of a front wheel skid the driver obviously has to release the brakes sufficiently to regain steering control and then apply again the brakes more gently. For a rear wheel skid, the driver steers in the direction the car is tending to point, thereby decreasing the upsetting torque, releasing the brakes, and reapplying them more gently. For a vehicle with front wheel drive the driver should in addition accelerate. The driver, of course, has to meet with no interference from other traffic and has to have sufficient road to carry out the required manoeuvre.

2.5 Adhesion Utilization

A vehicle wheel will start to lock when the braking force exceeds the product of the tire-road adhesion coefficient and the dynamic wheel load. The value of vehicle deceleration at this instant will be determined by the braking force on all the wheels, which in turn is determined by the braking distribution. The dynamic wheel load can be calculated from the deceleration and the static wheel load. It follows, therefore, that if the tire-road adhesion coefficient, the static wheel load distribution, and the braking distribution are all known, the safe limit of deceleration can be calculated. Since the ideal performance is obtained when the braking and dynamic load distribution are equal, the deceleration expressed as a proportion of "g" is in this case numerically

equal to the adhesion coefficient. A satisfactory method of examining the safe braking performance is to calculate the value of d/f, where

d = maximum safe deceleration

f = tire-road adhesion coefficient.

When the braking distribution is ideal, i.e. equal to the load distribution, then d/f = 1, the value of d/f has been called the "adhesion utilization", a term which correctly signifies its physical meaning. To study the braking performance of road vehicles, the following two criteria have to be examined:

1) the maximum deceleration that can be achieved without any wheel locking under varing loads, and road adhesion conditions; and
2) the variation in pedal effort required to produce a given deceleration due to changes in vehicle loading.

Figs. 2.5 - 2.9 show some typical vehicles and their adhesion utilization obtained for various tire-road adhesion coefficients under a fixed braking ratio [4]. The plots of d/f vs μ_A have been drawn for deceleration up to d = 0.6 for commercial vehicles and d = 0.87 for cars. These values of 'd' represent the maximum deceleration which can be employed without any damage due to load moving or passengers being thrown about.

In motorcycles, the front and rear brakes are operated independently by the rider, who is therefore able, in theory at least, to obtain any braking ratio he wishes. Fig. 2.10 shows the enormous changes in braking ratio of motorcycles that is required at the various decelerations if the dynamic weight ratio were to be equalled and achieve maximum

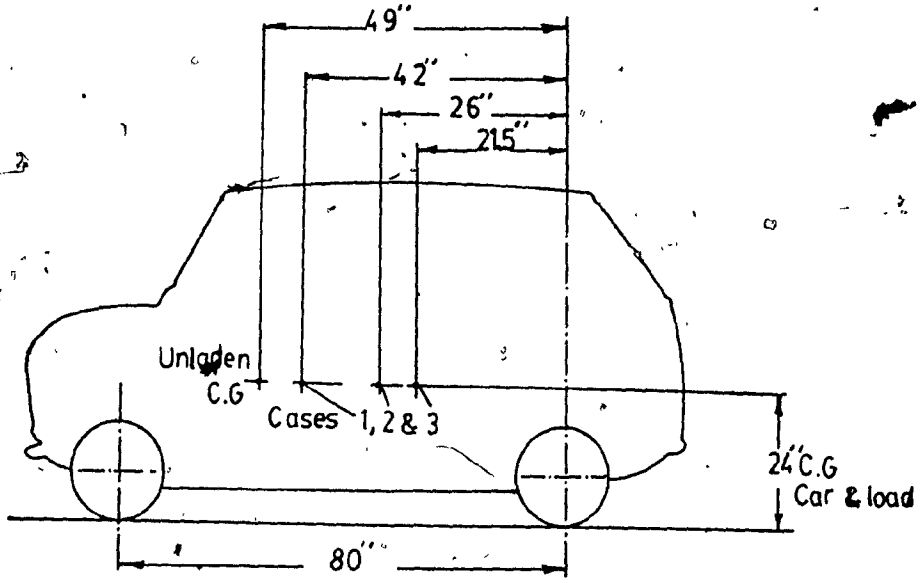

Fig. 2.5a - A Typical 12 CWT Passenger Car

Case 1 - Driver only, 1487 lb. G.V.W.

Case 2 - Driver, 1 front passenger & 150 lb. luggage, 1787 lb. G.V.W.

Case 3 - Driver, 3 passengers & 150 lb. luggage, 2087 lb. G.V.W.

Unladen Weight 1337 lb.

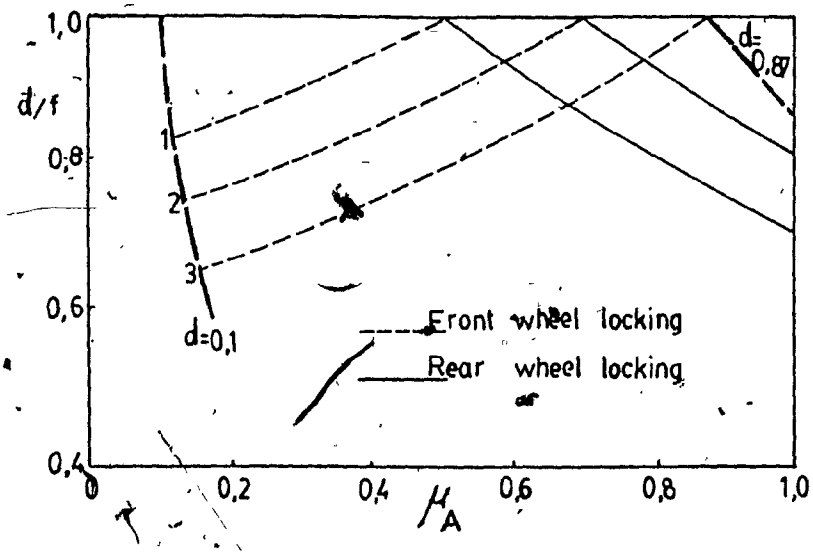

Fig. 2.5b - Plots of d/f Vs. μ_A for Deceleration d= 0.1 to 0.87 for 12 CWT Passenger Car

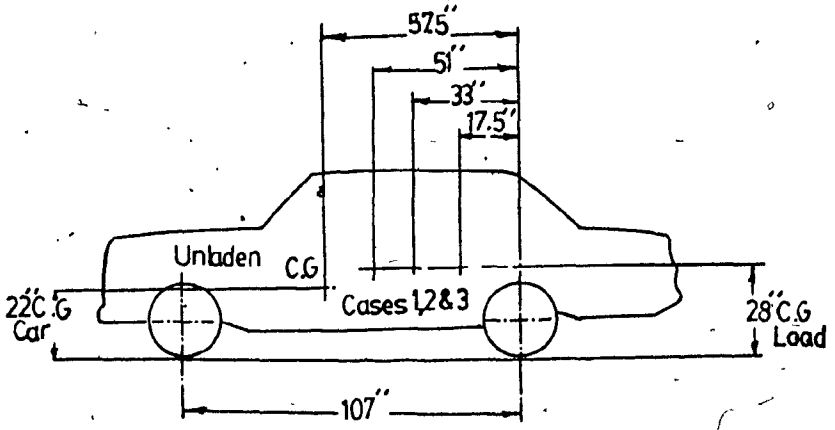

Fig. 2.6a - A Typical 25 CWT Passenger Car

Case 1 - Driver only, 2964 lb. G.V.W.

Case 2 - Driver, 2 front passengers & 150 lb. luggage, 3414 lb. G.V.W.

Case 3 - Driver, 3 rear passengers & 150 lb. luggage, 3564 lb. G.V.W.

Unladen Weight 2814 lb.

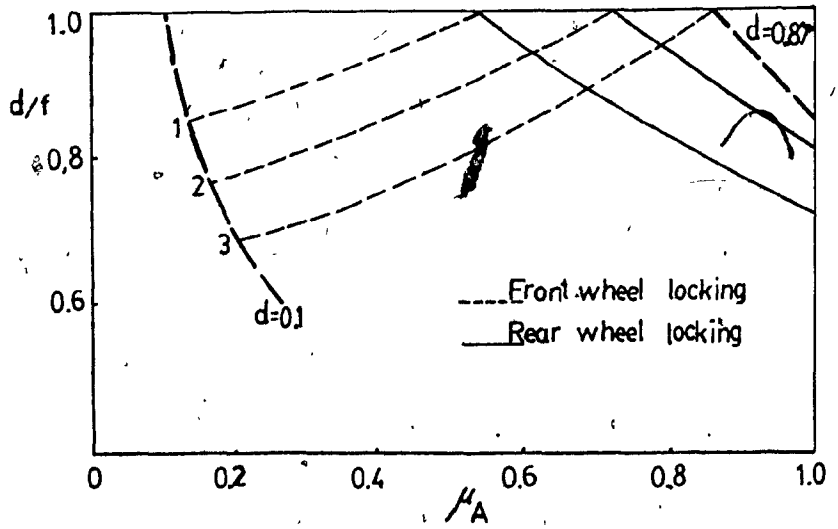

Fig. 2.6b - Plots of d/f Vs. μ_A for Deceleration d=0.1 to 0.87 for 25 CWT Passenger Car

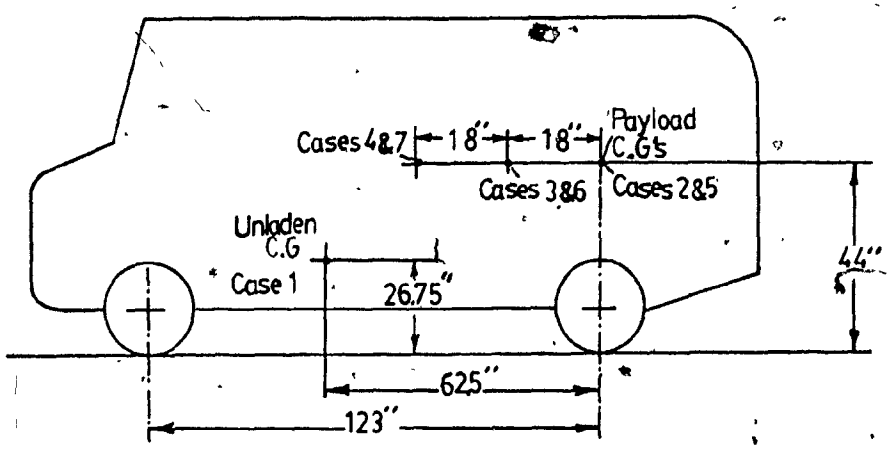

Fig. 2.7a - A Typical 2 Ton Van

Case 1 - Unladen, 4632 lb. G.V.W.
Case 2,3,4 - Half laden, 6872 lb. G.V.W.
Case 5,6,7 - Fully laden, 9112 lb. G.V.W.

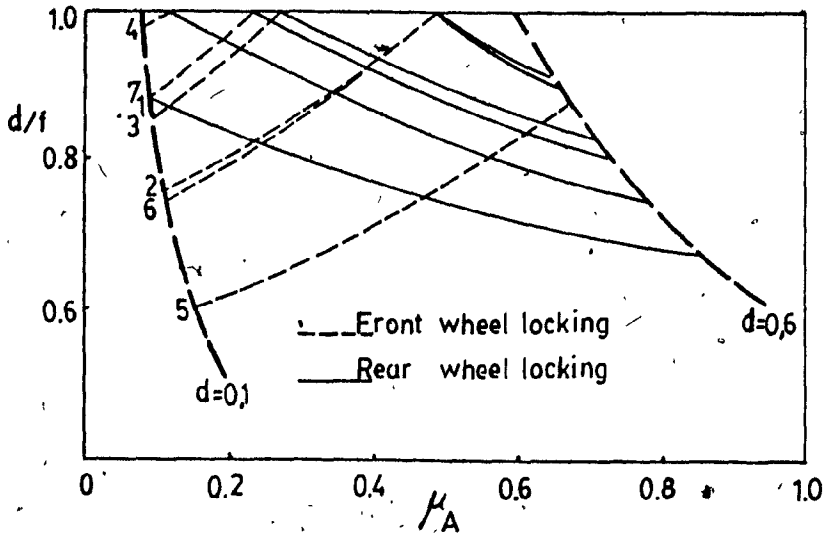

Fig. 2.7b - Plots of d/f Vs. μ_A for Deceleration d=0.1 to 0.6 for 2 Ton Van

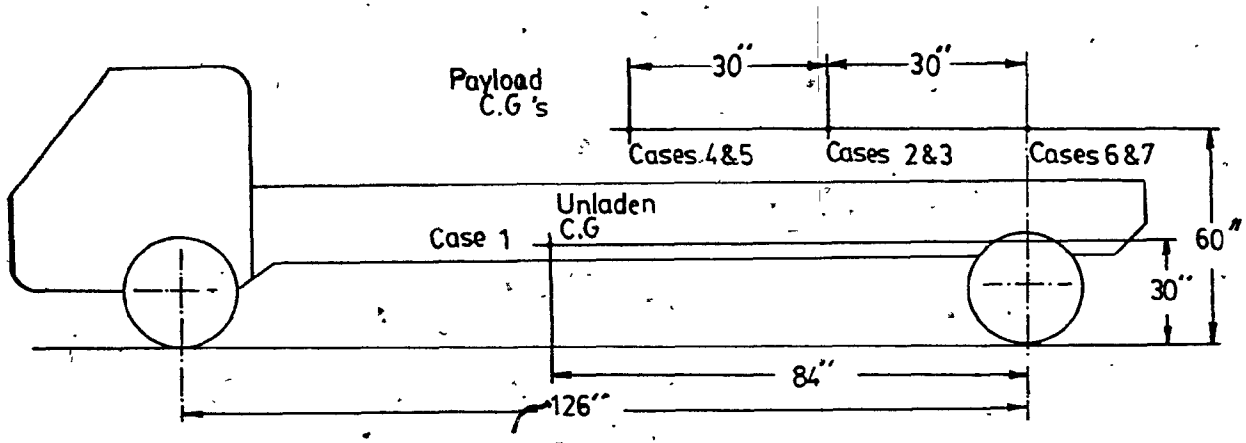

Fig. 2.8a - A Typical 7 Ton Commercial Vehicle

Case 1 - Unladen, 8514 lb. G.V.W.
Case 2,4,6 - Half laden, 17364 lb. G.V.W.
Case 3,5,7 - Fully laden, 26214 lb. G.V.W.

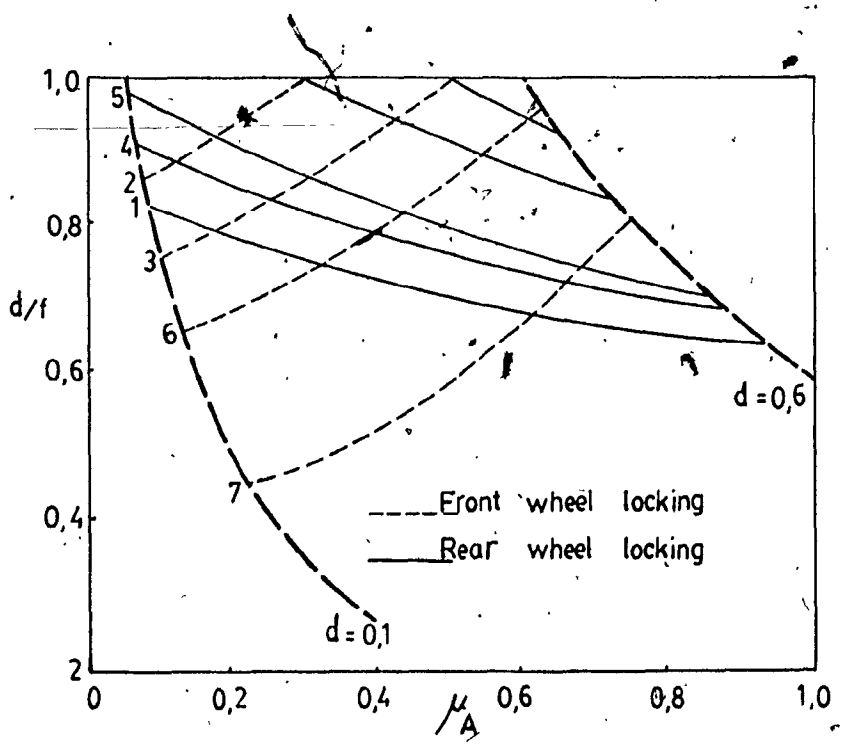

Fig. 2.8b - Plots of d/f Vs. μ_A for Deceleration d=0.1 to 0.6 for 7 ton Commercial Vehicle

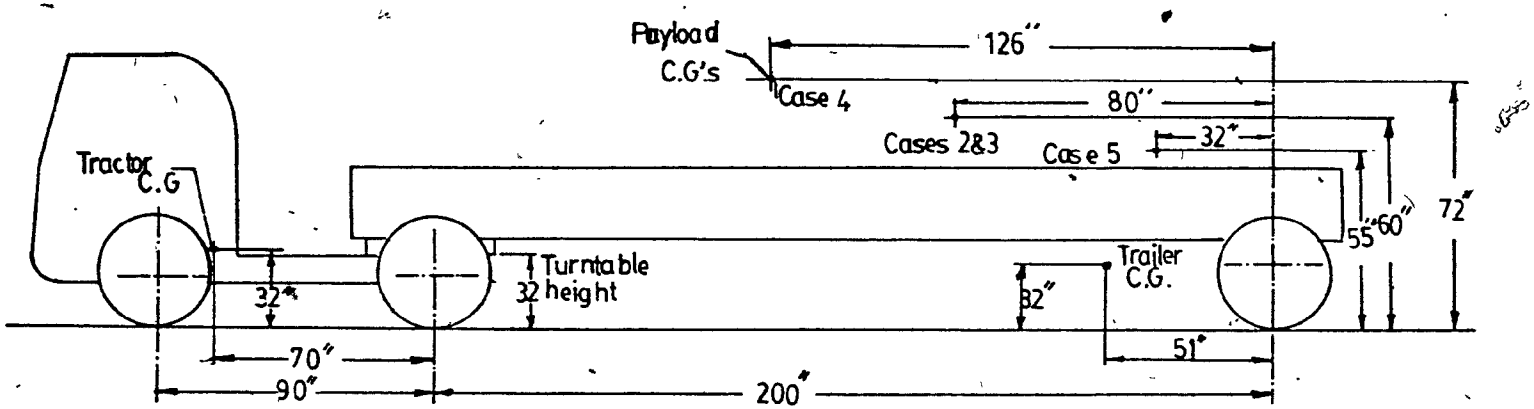

Fig. 2.9a - A Typical Articulated Commercial Vehicle

Tractor only		7924 lb. G.V.W.
Case 1 -	Tractor & Trailer unladen	13748 lb. G.V.W.
Case 2 -	Tractor & Trailer half laden,	27188 lb. G.V.W.
Case 3,4,5 -	Tractor & Trailer fully laden,	40628 lb. G.V.W.

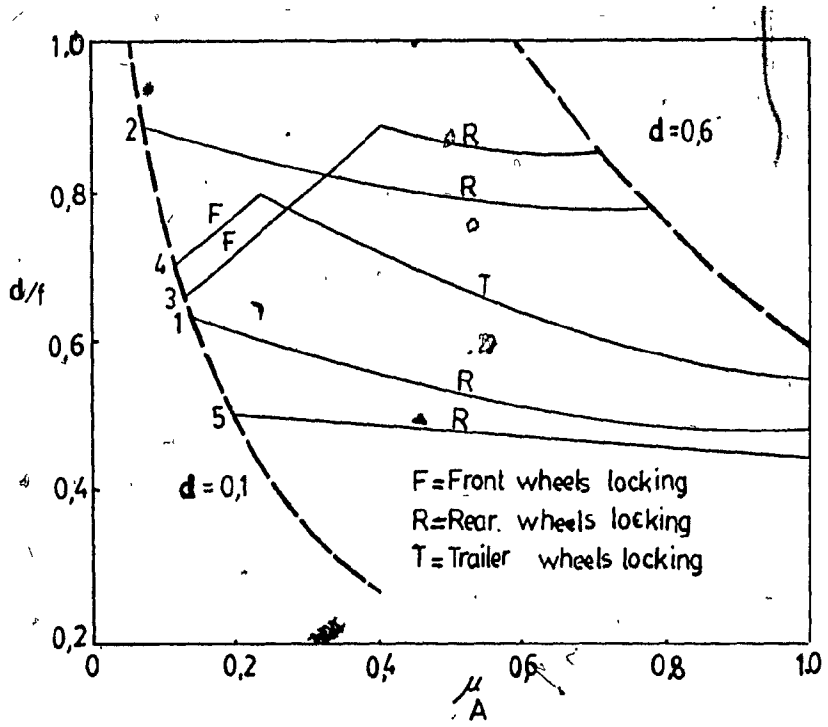

Fig. 2.9b - Plots of d/f Vs. μ_A for Deceleration d=0.1 to 0.6 for Articulated Commercial Vehicle

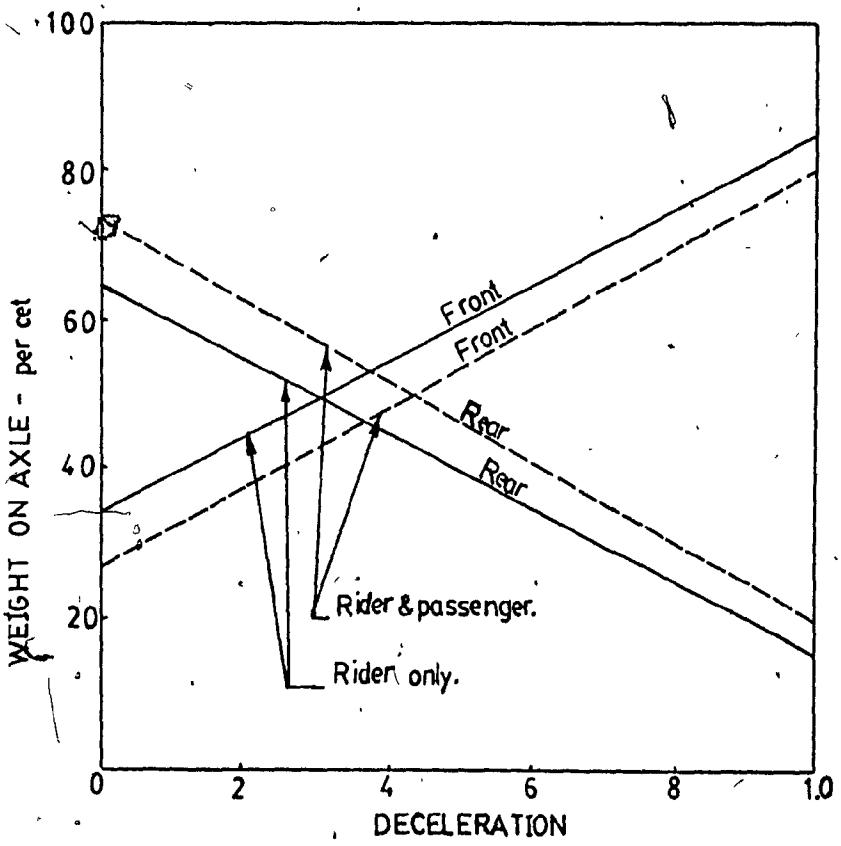

Fig. 10 - Wheel Loads on A Typical Motorcycle

braking. Since many motorcyclists do not use their brake for fear that the front wheel will lock, it can be seen how poor a deceleration will be achieved in these circumstances.

Deceleration is generally designed to be proportional to the pedal effort. The pedal effort is one factor which can be measured and which influences the gain that should be introduced into the braking system. Table 2.1 shows the variation in pedal effort that is required for a deceleration of 0.3g due to changes in load and illustrates the difference between cars and commercial vehicles in this respect.

2.5.1 Apportioning Valves

The simplest method of modifying the conventional fixed-ratio braking distribution is to add a pressure modulating valve in the rear brake line. Three basic types of such valves are available [4] and each can be manufactured with pressure-limiting or pressure-reducing characteristics.

(i) Deceleration conscious valves (D.C.V.)— It is a valve which uses the inertia force of a suspended mass to vary the braking ratio. The D.C.V. has no effect on static weight changes and can therefore only be used on those passenger cars where static axle weights do not substantially change. Valves using this principle have been designed, but none are in production use.

(ii) Pressure conscious valves— Since the brake line pressure is approximately proportional to the deceleration for a particular gross vehicle weight, a pressure limiting valve which limits the pressure to the rear brakes can be used to increase the braking ratio at higher deceleration. These valves are most useful in cars of short wheel base since this type of valve are of the greatest benefit where weight transfer is greatest.

Table 2.1 -- The Variation of Pedal Effort and Its Ratio in Terms of Different Type of Vehicles [4].

Vehicle	Pedal Effort for 0.3g Deceleration, lb		Ratio of Pedal Effort
	Unladen & Driver	Laden	Laden/Unladen
12 cwt car	31.5	44.5	1.4
25 cwt car	22.5	29	1.3
2 ton van	33	65	2.0
7 ton C.V.	20	44	2.2
Articulated C.V.	19	40	2.1

A benefit of this type of valve is that the limiting valve has enabled the incidence of rear wheel locking to be reduced without depending on adhesion utilization. This valve, however, is unsuitable where large change in loading can occur over the rear axle. A further disadvantage of pressure limiting valve is the high pedal efforts required when the vehicle is laden.

(iii) Load conscious valves — The most direct way of achieving a high adhesion utilization is to use a valve which will alter the braking distribution according to the load as measured by the deflection of the spring or the pressure in an air suspension chamber. If such a valve has a fast enough response, it will allow the braking distribution to follow the load distribution both on static weight changes and on load transfer.

It is highly unlikely that such a device has been developed which would yield such a perfect response. The major application is for commercial vehicles, on which the axle weights can vary by a factor of five or six, but if the response is adequate, it will be equally useful for passenger cars.

The relevant advantage between the above types have to be balanced between the performance achievement level and the cost-simplicity of design and installation on any particular vehicle.

The load conscious pressure-reducer provides the best performance but is the most expensive and the linkage is vulnerable to damage and maladjustment. In practice, lining friction coefficient may become extremely critical; a car fitted with a variable-ratio system matched to prevent rear-wheel locking through the adhesion range could be very adversely affected by a slight increase in rear brake lining effectiveness. Thus the potentially safe system could then exhibit a greater

degree of instability.

2.5.2 The Effect of Apportioning on Adhesion Utilization

Fig. 2.11 shows the improved adhesion of utilization and the absence of rear-wheel locking when an apportioning valve is added. In fact, it is often possible to achieve in excess of 80 per cent utilization over a very wide range of adhesion conditions from dry concrete to wet ice. Unfortunately, the great limitation of all such apportioning devices is that the brake system itself cannot prevent the driver ultimately exceeding the maximum safe deceleration and then locking the wheels.

2.6 Increase of Braking Size

When apportioning valves are fitted to each axle, good adhesion utilization and a satisfactory pedal effort will be obtained. However, they have some serious disadvantages. The proportion of energy dissipated at each brake will no longer be fixed and so large brakes will have to be fitted to ensure that severe fade and excessive wear are not encountered. If total apportioning is used, the braking ratio can vary from 20/80 for low decelerations on a vehicle with a full load placed over the rear axle to 60/40 for 0.5g decelerations on an unladen vehicle or a vehicle whose load is well forward. The effect of this on temperature variation will be extremely large. Fig. 2.12 shows the temperatures which are likely to be encountered when brakes designed for a fixed braking ratio of 50/50 are used at other ratios to dissipate at the same total energy rate. The effect of these changes of temperature on the lining wear rate are also shown.

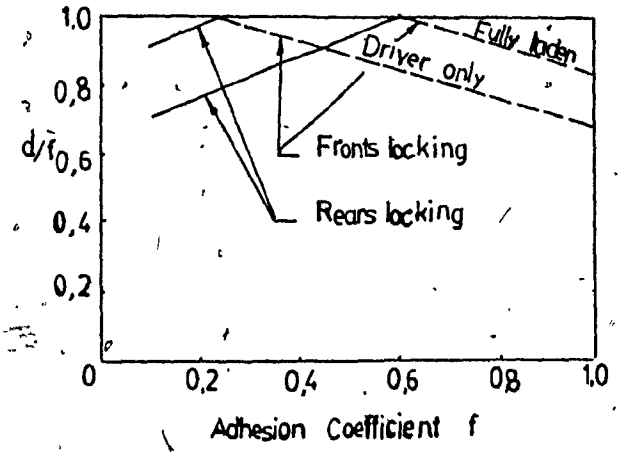

Fig. 2.11a - Effect of Apportioning on Adhesion Utilization (Fixed Braking Ratio-No Valve)

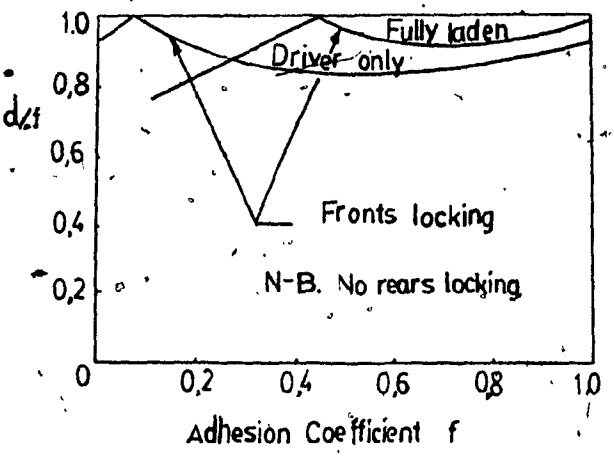

Fig. 2.11b - Effect of Apportioning on Adhesion Utilization (Variable Braking Ratio Apportioning Valve Fitted)

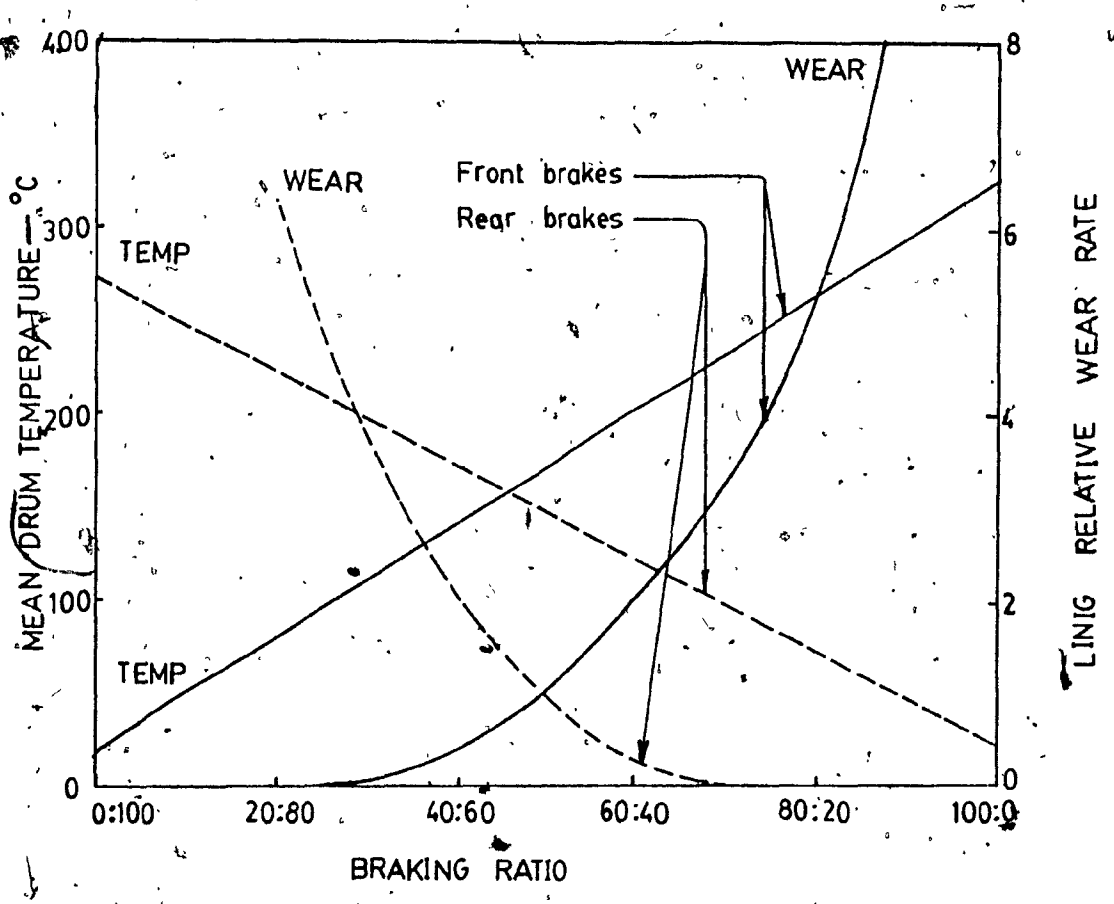

Fig. 2.12 - Temperature and Rate for Varying Braking Ratio for the 7 Ton Commercial Vehicle

The extreme braking ratios will only occur with badly loaded vehicles, but it will be necessary to ensure that the wear of either brake will not be too rapid in any uniformly laden vehicle. At present it is common practice to fix the braking ratio by the braking that is required to decelerate a uniformly laden vehicle at 0.6g. Since most work is done at decelerations of less than 0.2g it may be necessary to marginally increase the size of the rear brake to account for the greater proportion of braking on the laden vehicle at this lower deceleration. It may be necessary to increase the size of the front brake to allow for the extra energy that will be dissipated at that brake on the lightly laden or unladen vehicle due to the high, front-rear braking ratio.

2.7 Load Compensation

It has already been pointed out that for a particular vehicle the pedal effort required to give a fixed deceleration will be substantially proportional to the gross vehicle weight. Since commercial vehicle commonly have a laden weight which is between two and three times the unladen weight, the very light pedal effort required to brake an unladen vehicle on a slippery road will lead to considerable danger of loss of control. To overcome this, the devices already considered for altering the braking distribution according to the axle load can be made to alter the pedal effort brake torque relationship without affecting the fixed braking ratio. This is achieved by using one valve or variable booster on the rear axle [4]. The use of the variable booster is particularly applicable to light commercial vehicles, since many of those already employ a vacuum booster to assist the hydraulic actuation. Fig. 2.13 shows the adhesion utilization for fully apportioned vehicle when two

variable output boosters are used. Now in order to study the effects of load compensation two categories of vehicles need to be considered:

(1) vehicles whose braking system are direct hydraulic without assistance (generally 2 tons pay load weight and under); and

(2) vehicles which at present use a vacuum booster.

To obtain the maximum improvement in the control of braking, a variable output booster should obviously be fitted to each axle on both classes of vehicles. However, if for other reasons only one such booster is used, the choice must be made whether to use it to operate the rear brake only, thereby giving partial apportioning, or to operate all the brakes, i.e. as a load compensator. On a vehicle of the first category it will probably be preferable to use it to operate the rear brakes only, since this will improve both the adhesion utilization and the pedal effort as shown in Fig. 2.14 and 2.15. On vehicles of the second category it must be used to operate all the brakes, otherwise the system cannot fully meet the requirements of braking a fully laden vehicle for which the original booster was employed. In this case, the boost ratio is being reduced and the pedal effort increased for the lightly laden vehicle.

2.8 Safety and Reliability

With road giving adhesion coefficients varying from f = 0.2 in wet and icy conditions to f = 1.0 in dry surface, there is a big scope for the improvement in the deceleration obtained without wheel locking. Any unreliability in the performance of the device could consequently lead directly to an increase in the number of accidents. Brakes are

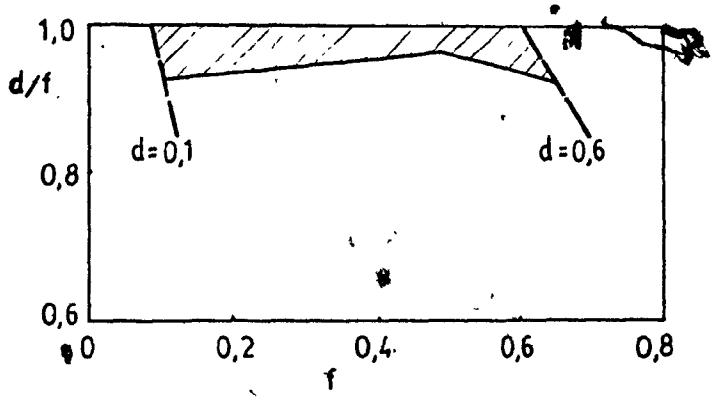

Fig. 2.13 - Adhesion Utilization for Fully Apportioned Vehicle Using 2 Variable Output Boosters for 2 Ton Van

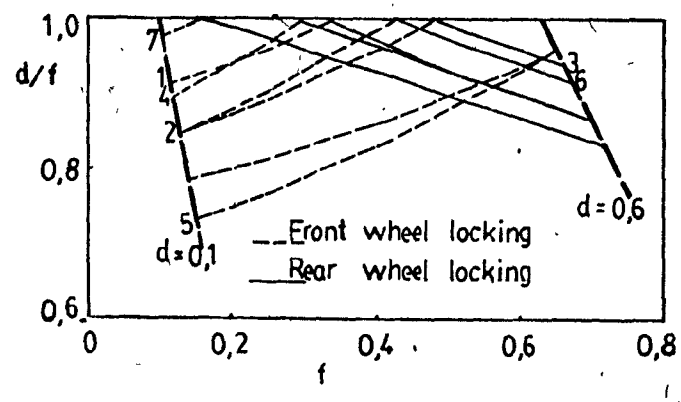

Fig. 2.14 - Adhesion Utilization When Varaible Output Booster Is Fitted to Rear Axle Only for 2 Ton Van

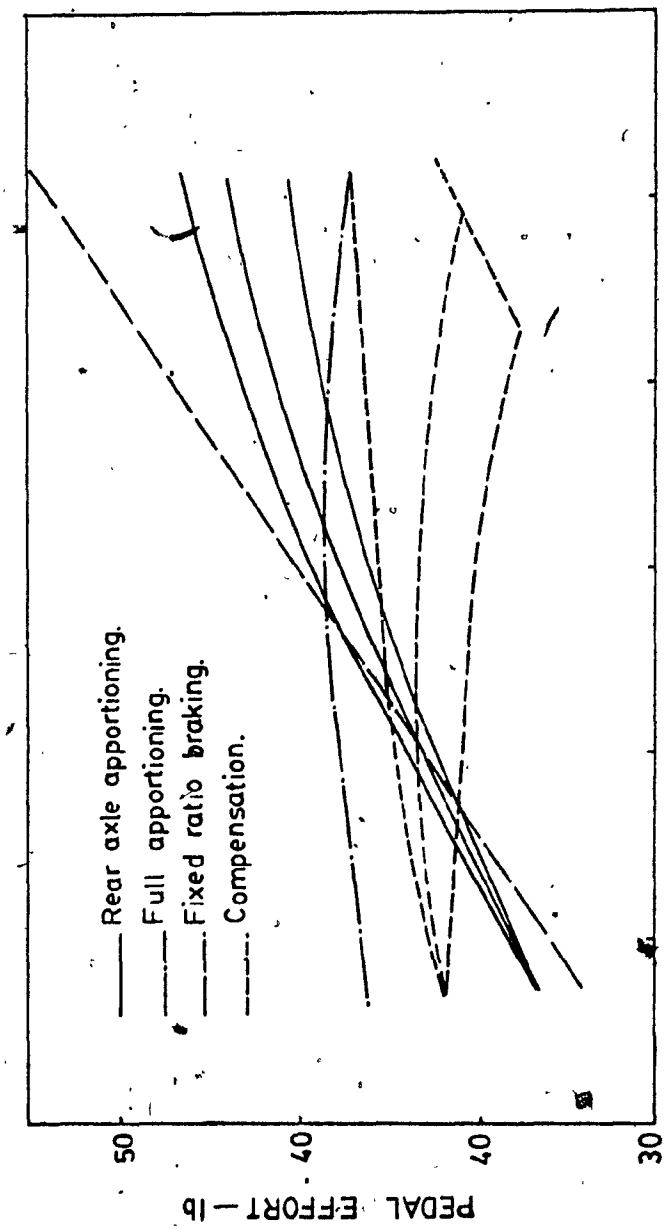

Fig. 2.15 - Variation in Pedal Effort Required to Produce a Deceleration of 0.3 g. for 2 Ton Van

designed with the maximum reliability in mind, using the least number of complications. However, high deceleration on a poor road surface is the ultimate test for the insufficiency in the braking ratio, in which case the driver will probably be in serious trouble if some wheels lock. Therefore, any device which limits wheel locking and allows greater deceleration to be used, must be so simple that any possibility of unreliability can be discounted, or it must function every time when the brakes are used so that the driver will be aware if it ceases to work efficiently.

2.9.1 Prevention of Vehicle Spin

Stark and Lister [22] showed that the incidence of vehicle spin during emergency braking of cars could be stopped by locking the front wheels before the rear wheels. This should also hold true for commercial vehicles. The load conscious valves can easily be set to give a little more braking at the front than would be chosen for maximum adhesion utilization, so ensuring that the front wheels lock first, preventing vehicle spin. The loss of adhesion utilization is small, probably much less than the loss of utilization when the pressure limiting valve is used on passenger cars.

CHAPTER 3

DYNAMICS OF VEHICLES UNDER THE ACTION OF BRAKING

3.1 GENERAL

During the accelerating or braking phase of vehicle performance, the handling characteristics may vary considerably from those obtained from steady speed conditions. In certain cases, the dynamic change in the vehicle can be utilized to enhance some particular aspect of handling. For example, the application of an accelerating force through the rear wheels of a rear drive vehicle is a means whereby lateral responses may be increased. The braking process can in extreme cases result in either complete loss of directional control, with the result that the vehicle moves in a manner which is solely dependent on its attitude immediately prior to brake application, or alternatively in absolute stability in which the vehicle cannot deviate from a straight line motion. Either condition is potentially dangerous, and certainly undesirable.

The description of emergency conditions involving heavy braking or acceleration, or sudden manoeuvers are not well described by steady state solution or linearized systems of forces. Therefore, we need to find transient type solution to deal completely with vehicle behaviour under such conditions. Available literature on transient behaviour of vehicles during braking is limited. Often these works are based on a

simple mathematical model of the vehicle and ignoring the vertical motion of the car or unequal brake action or using a mathematical model with a simple two-wheel system.

3.2 A Simplified Model of Vehicles in Dynamic Study

3.2.1 Mathematical Model

Pacejka [23] has developed the dynamic equation of motion of an automobile undergoing unrestricted motion in six degrees of freedom by retaining only those terms that are invariant in time. He has also made the following additional assumptions in order to obtain the equations:

(1) The wind velocity is assumed to be zero relative to ground but a drag force due to air resistance, wind force is assumed to act at the origin of the axis system, ξ_s, ζ_s, η_s point, Ω, Fig. 3.1.

(2) The effects of drive shaft torque, T, have been added.

(3) The angle, λ, is assumed to be small so that

$$\sin \lambda = \frac{z_2}{\ell} \quad \text{and} \quad \cos \lambda = 1$$

(4) All products involving $(z_2/\ell)\phi_{1,2}$ have been considered negligible and have, therefore, been omitted.

Based on the above assumptions, the dynamic equations of motion of an automobile is given by:

$$-M\dot{y}\dot{\psi} = X_1 + X_2 + X_w \quad \ldots\ldots\ldots\ldots\ldots \quad (3.1)$$

$$M\dot{x}\dot{\psi} - M_s \{ e\phi + \frac{z_2}{\ell}(a-c) \} \psi^2 = Y_1 + Y_2 \quad \ldots\ldots\ldots \quad (3.2)$$

$$M_s \{ e\phi + \frac{z_2}{\ell}(a-c)\phi_2 \} \dot{y}\dot{\psi} = aY_1 - bY_2 + N + X_t \quad \ldots\ldots \quad (3.3)$$

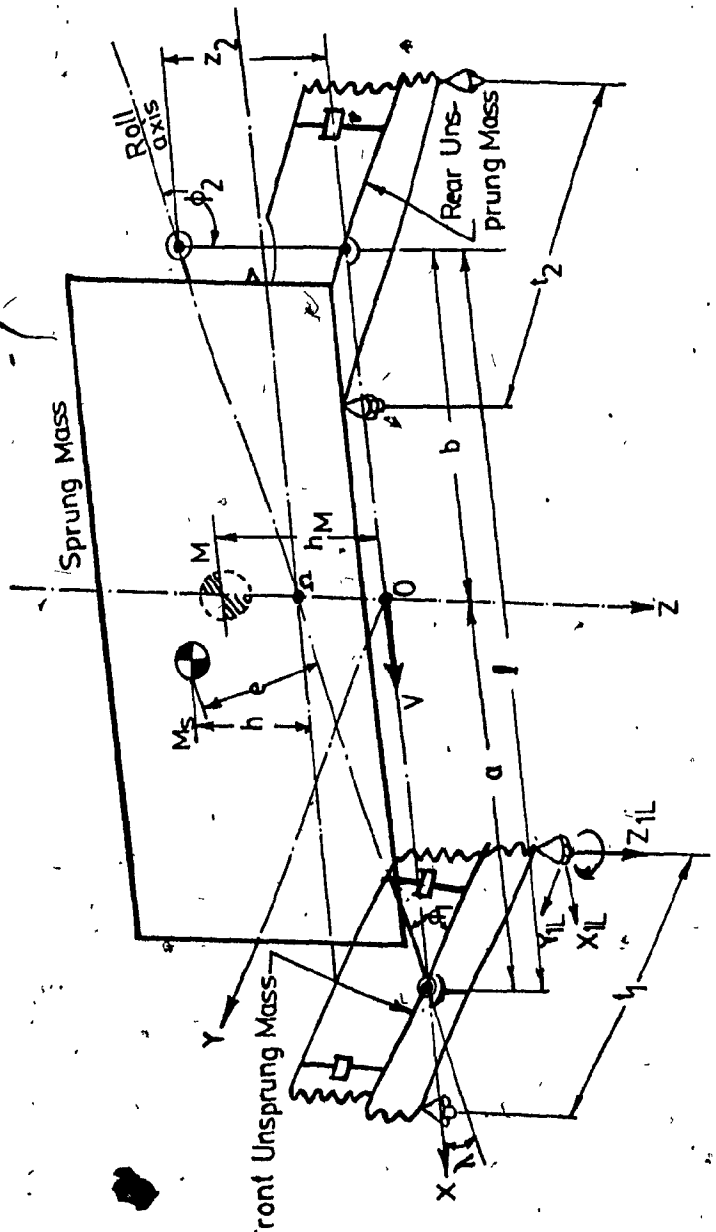

Fig. 3.1 - Representative Configuration of an Hypothetical Automobile

$$M_s e\left(\dot{x}\dot{\psi} - a\frac{z_2}{l}\phi_2\psi^2 - \frac{z_2}{l}\phi_2\dot{\psi}\dot{y} + \frac{z_2}{l}\phi\dot{y}\dot{\psi}\right) - M_s ge\phi - T$$

$$+(I_{\zeta_s} - I_{\eta_s} + \frac{z_2}{l}C_{\zeta\xi})\dot{\psi}^2\phi + k_1(\phi-\phi_1) + k_2(\phi-\phi_2) = (N+N_t)\frac{z_2}{l} \quad \ldots (3.4)$$

$$- k_1(\phi-\phi_1) + B_1(\phi_1) = 0 \quad \ldots (3.5)$$

$$M_s\frac{z_2}{l}\{\dot{x}\dot{\psi}(a-c) - e\phi\dot{y}\dot{x} - ac\phi\dot{\psi}^2\} + M_u z_2\dot{x}\dot{\psi} + T + B_2(\phi_2)$$

$$- \{M_s(\frac{a-c}{l}) + M_{u_2}\}gz_2\phi_2 - k_2(\phi-\phi_2) - M_s h\frac{z_2}{l}\phi_2\dot{\psi}\dot{y}$$

$$+ C_{\zeta\xi}\frac{z_2}{l}\phi_2\dot{\psi}^2 = -(N + X_t)\frac{z_2}{l} \quad \ldots (3.6)$$

where

$$X_{2R} = X_{1L} + X_{1R} \qquad X_{1R} = X_{2L} + X_{2R}$$

$$Y_{2R} = Y_{1L} + Y_{1R} \qquad Y_{1R} = Y_{2L} + Y_{2R}$$

$$N = N_{1L} + N_{1R} + N_{2L} + N_{2R}$$

$$X_t = \frac{t_1}{2}(X_{1L} - X_{1R}) + \frac{t_2}{2}(X_{2L} - X_{2R}) \quad \ldots (3.7)$$

Assuming that there is no loss between the engine and the rear tire due to gear inefficiency, friction, etc., then the drive-shaft torque can be written as:

$$T = \frac{r}{\eta}P_{th} \quad \ldots (3.8)$$

where

$$P_{th} = P_{2L} + P_{2R}$$

The wind force, X_w, can be written as

$$X_w = -\frac{1}{2}C_w A_r \upsilon \dot{x}|\dot{x}| \quad \ldots (3.9)$$

The rolling stiffness about the roll axis of the sprung mass is a function of the spring suspension system which exists between the body sprung mass and the front and rear axle masses. The moments produced by these spring elements will therefore be a function of the relative angular displacements of these masses about their respective roll axes. These relative displacements are $(\phi - \phi_1)$ and $(\phi - \phi_2)$. Experimental curves of roll moment versus relative roll displacement for a typical American passenger automobile indicate a central linear portion, the upper and lower limits being $+\phi'_{1,2}$ and $-\phi'_{1,2}$, respectively, and non-linear outer portions whose extreme upper and lower limits are $+\phi''_{1,2}$ and $-\phi''_{1,2}$ respectively. These characteristics can be approximated by the following mathematical expressions:

$$k_{1,2}(\phi - \phi_{1,2}) = a_{1,2}(\phi - \phi_{1,2}) \qquad -\phi'_{1,2} \leq (\phi - \phi_{1,2}) \leq \phi'_{1,2}$$

$$k_{1,2}(\phi - \phi_{1,2}) = a_{1,2}\left[\phi'_{1,2} + \frac{2}{\pi}(\phi''_{1,2} - \phi'_{1,2}) \times \tan\left\{\frac{(\phi - \phi_{1,2} - \phi'_{1,2})}{\phi''_{1,2} - \phi'_{1,2}} \frac{\pi}{2}\right\}\right] \qquad \phi'_{1,2} < (\phi - \phi_{1,2}) < \phi''_{1,2}$$

$$k_{1,2}(\phi - \phi_{1,2}) = \infty \qquad \phi''_{1,2} < (\phi - \phi_{1,2}) \quad \ldots\ldots \quad (3.10)$$

where $a_{1,2}$ is the coefficent for rolling moments on the sprung mass, front and rear, respectively.

$$k_{1,2}(\phi-\phi_{1,2}) = a_{1,2}\left[-\phi'_{1,2} + \frac{2}{\pi}(\phi''_{1,2} - \phi'_{1,2}) \right.$$

$$\left. \text{Xtan}\left\{\frac{(\phi-\phi_{1,2}) + \phi'_{1,2})}{\phi''_{1,2}-\phi_{1,2}} \frac{\pi}{2}\right\}\right] \qquad -\phi''_{1,2} < (\phi-\phi_{1,2}) < -\phi'_{1,2}$$

$$k_{1,2}(\phi-\phi_{1,2}) = -\infty \qquad (\phi-\phi_{1,2}) < -\phi''_{1,2}$$

The rolling moments on the unsprung masses, about the front and rear roll axes, respectively, $B_{1,2}$ are given by the expressions:

$$\left.\begin{aligned} B_{1,2}(\phi_{1,2}) &= -A_{1,2} && k_s\left(\frac{t_{1,2}^2}{2}\right)\phi_{1,2} < -A_{1,2} \\ B_{1,2}(\phi_{1,2}) &= K_s\left(\frac{t_{1,2}^2}{2}\right)\phi_{1,2} && k_s\left(\frac{t_{1,2}^2}{2}\right) |\phi_{1,2}| \leq A_{1,2} \\ B_{1,2}(\phi_{1,2}) &= A_{1,2} && k_s\left(\frac{t_{1,2}^2}{2}\right)\phi_{1,2} > A_{1,2} \end{aligned}\right\} \quad \ldots\ldots (3.11)$$

where

$$A_1 = \frac{t_1}{2\dagger}(Mgb + Mh_m\dot{y}\,\dot{\psi} + I_{zx}\,\dot{\psi}^2)$$

$$A_2 = \frac{t_2}{2\dagger}(Mga - Mh_m\dot{y}\,\dot{\psi} + I_{zx}\,\dot{\psi}^2) \quad \ldots\ldots\ldots\ldots\ldots\ldots (3.12)$$

and $B_{1,2}$ is the rolling moment of the unsprung masses about the front and rear roll axes respectively.

The slip angles of the tires are given by the expression:

$$\alpha_{ij} = \beta_{ij} - \gamma_{ij} \quad \ldots\ldots\ldots\ldots\ldots\ldots (3.13)$$

where

$$\tan\beta_{1L} = \frac{\dot{y} + a\,\dot{\psi}}{\dot{x} + (t_1/2)\,\dot{\psi}}$$

$$\tan\beta_{1R} = \frac{\dot{y} + a\dot{x}}{\dot{x} - (t_1/2)\,\dot{\psi}} \qquad \ldots\ldots\ldots\ldots\ldots\ldots \quad (3.14)$$

$$\tan\beta_{2L} = \frac{\dot{y} - b\dot{\psi}}{\dot{x} + (t_2/2)\,\dot{\psi}}$$

$$\tan\beta_{2R} = \frac{\dot{y} - b\dot{\psi}}{\dot{x} - (t_2/2)\,\dot{\psi}}$$

$$\gamma_{ij} = \delta_{ij} + \alpha_{ij}$$

δ_{ij}, the input steer angles, are zero for the two rear wheels and the expression for the two front wheels is given by:

$$\text{cotan}\,\delta_{1L} = \text{cotan}\,\delta_{1R} + t_1/l \qquad \ldots\ldots\ldots\ldots \quad (3.15)$$

Assuming an Ackerman steering layout, the average input steer angle, , is defined by the equation

$$\delta = (\delta_{1L} + \delta_{1R})/2 \qquad \ldots\ldots\ldots\ldots \quad (3.16)$$

Fiala [24] has derived the following expressions for the tire side force. The tire side force (F_{ij}) is a function of the slip angle, camber angle, vertical load, friction coefficient and longitudinal force and is expressed by the following equation:

$$F_{ij} = C_{cij}\,\theta_{ij} + 3/2\left(\sqrt{Z_{ij}^2 f^2 - W_{ij}^2} \mp C_{cij}\theta_{ij}\right)\left(-y_{ij} \mp \frac{y_{ij}^2}{2} - \frac{y_{ij}^3}{12}\right)$$

for

$$|y_{ij}| < 2 \quad \text{and} \quad \alpha_{ij} y_{ij} > 0 \qquad \ldots\ldots\ldots\ldots\ldots\ldots \quad (3.17)$$

and

$$F_{ij} = -(\pm)\sqrt{Z_{ij}^2 f^2 - W_{ij}^2} \qquad \ldots\ldots\ldots\ldots\ldots\ldots \quad (3.18)$$

for

$$|y_{ij}| > 2 \quad \text{or} \quad \alpha_{ij} y_{ij} < 0$$

where

$$i = 1, 2, \quad \text{and} \quad j = \text{left, right}$$

and

$$y_{ij} = \frac{c_{ij} \tan \alpha_{ij}}{3/2\left(\sqrt{Z_{ij}^2 f^2 - W_{ij}^2} \pm C_{cij}\,\theta_{ij}\right)} \qquad \ldots\ldots\ldots \quad (3.19)$$

In equation (3.17), (3.18) and (3.19), the negative signs are used for $\alpha_{ij} < 0$ and the positive signs for $\alpha_{ij} > 0$.

Each longitudinal tire force, W_{ij}, is the sum of the rolling resistance and the traction force on the tire. These forces are expressed as follows:

$$W_{ij} = -Z_{ij}\,(A' + B' v_{ij}) \qquad \ldots\ldots\ldots\ldots\ldots\ldots \quad (3.20)$$

where A', B' are the coefficient of rolling resistance.

$$W_{2j} = (P_{th}/2) - Z_{2j}(A' + B'v_{2j})$$

for

$$(P_{th}/2) - Z_{2j}(A' + B'v_2) < Z_{2j}f$$

and

$$W_{2j} = \mu_{2j}f$$

for

$$(P_{th}/2) - Z_{2j}(A' + B'v_{2j}) \geq Z_{2j}f \quad \ldots\ldots\ldots\ldots\ldots\ldots (3.21)$$

where

$$v_{1j} = \sqrt{(\dot{y} + a\dot{\psi}^2) + \{\dot{x} \pm (t_1/2)\dot{\psi}\}^2} \quad \ldots\ldots\ldots\ldots\ldots (3.22)$$

$$v_{2j} = \sqrt{(\dot{y} - b\dot{\psi})^2 + \{\dot{x} \pm (t_2/2)\dot{\psi}\}^2} \quad \ldots\ldots\ldots\ldots\ldots (3.23)$$

and the positive sign is used for j = left, the negative sign for j = right. In deriving the above equations, it was assumed that the automobile is rear drive and has a conventional differential which divides the torque equally to the two rear wheels.

The vertical load on each wheel is given by the equation

$$Z_{ij} = \frac{1}{t_{1,2}} \{A_{1,2} \pm B_{1,2}(\phi_{1,2})\} \quad \ldots\ldots\ldots\ldots\ldots (3.24)$$

where the negative sign is used for j = left, the positive sign is used for j = right, and $B_{1,2}(\phi_{1,2})$ and $A_{1,2}$ are given by equation (3.11) and (3.12), respectively.

Fig. 3.2 shows the various forces acting on the tire and the various angle that are pertinent to creation of these forces and their further resolution to vehicle axes. Examination of Fig. 3.2 shows that the X and Y forces prodcued by each wheel are:

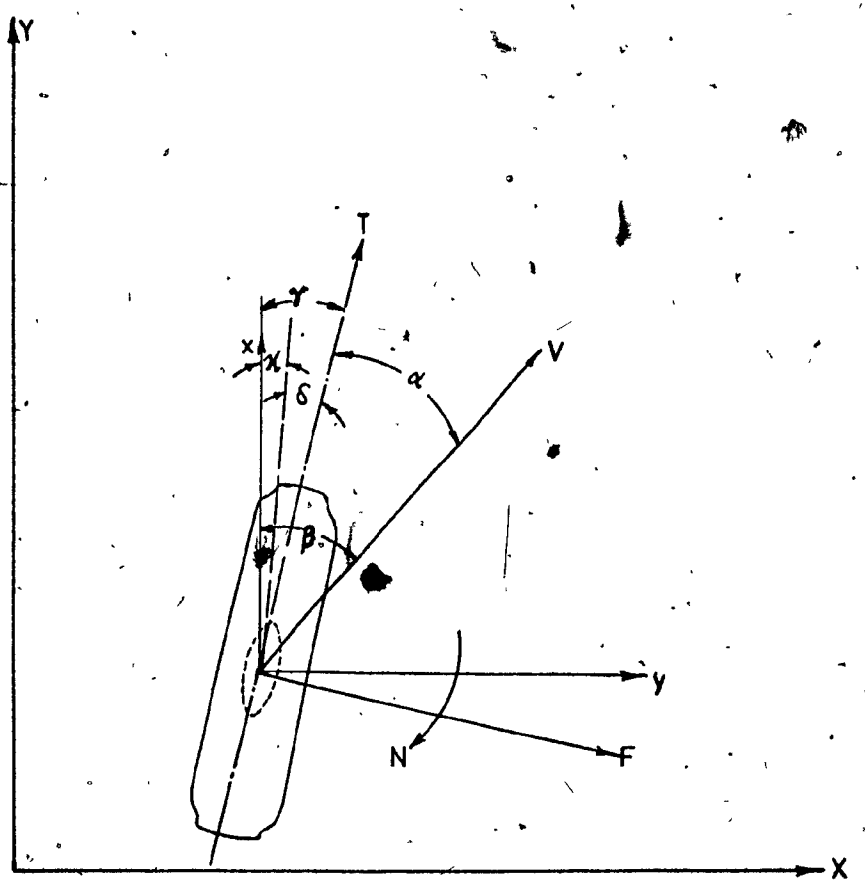

Fig. 3.2 - Diagram of Wheel Forces and Angles

$$\left.\begin{aligned} X_{ij} &= W_{ij} \cos \gamma_{ij} - F_{ij} \sin \gamma_{ij} \\ Y_{ij} &= W_{ij} \sin \gamma_{ij} + F_{ij} \cos \gamma_{ij} \end{aligned}\right\} \quad \ldots\ldots\ldots\ldots \quad (3.25)$$

3.2.2 Solution Methodology of the Simplified Vehicle Model

The preceding sets of non-linear equations cannot be solved straightforward, because of the intricacy of the simultaneous non-linear algebraic and transcendental equations that make up the mathematical model of the vehicle and tire. The Newton-Raphson Method [24], was used to solve these non-linear equations numerically. With this method, one assumes initial or "starting" values of the six primary response variable ($\dot{x}$, $\dot{y}$, $\dot{x}$, ϕ_1, and ϕ_2), performs a series of calculations using the equations (3.1) to (3.25) (e.g. for the slip angles, camber angles, tire forces and moments), and then checks the accuracy of the initial values by calculating all of the terms in the equilibrium equations. The left-hand side and right-hand sides of these equations will then differ from zero by a set of numbers which are called residuals.

Following the Newton-Rapson method these residuals are used to arrive at improved approximations for the six primary response variables. The entire process is repeated using successively improved approximations until finally, a point is reached where all of the response variables of the automobile and types may be computed with sufficient accuracy.

The drag force X_w, depends only on the magnitude of the longitudinal velocity of the vehicle, and its magnitude is negligible. The longitudinal force on each tire is taken as the difference of the thrust on the tire and the rolling resistance of the tire. Since the assumed automobile is driven at the rear through a differential, the thrust at

the front wheels is zero while the thrust at each rear wheel is one-half of the total applied thrust, P_{th}.

The vertical load on each tire is determined by the weight distribution of the standing automobile and by the magnitude of the load transferred from side to side and from front to rear.

Rolling moments, about the roll axis, are applied to both the sprung and unsprung masses. These moments are assumed to be non-linear functions of the relative roll displacement between the sprung and unsprung masses.

The slip angle, α, at each wheel is the difference between the angle β (between the reference longitudinal axis, X, of the vehicle and the velocity of the axle relative to the grounnd) and the total steer angle, V. This steer angle is the sum of the input steer angle and the toe change, χ. Toe changes, both front and rear, are caused by roll steer and were represented by empirical equations derived by fitting a curve to experimental datas for a typical automobile.

From the above discussion, it is apparent that mathematical model is restricted in the sense that the equations represent characteristics of one specific tire for one inflation pressure. The following specific set of vehicle characteristics have been specified in order to simplify calculations:

(a) 55 per cent of the weight of the car is carried by the front wheels

(b) the driving wheels are at the rear of the car

(c) the front roll stiffness has been increased by the use of an anti-roll bar, to a value that is approximately three times the rear roll stiffness.

3.2.3 Results and Discussion

Some of the results obtained from the analysis are presented in this section. Further discussions on the relationship between path curvature responses and vehicle handling characteristics are also presented. The results for the vehicle responses and tire forces are obtained for steer angle of 1, 2, 4, 8 and 16 degrees and for values of thrust from 0 to 1100 lb.

Figure 3.3 illustrates the non-linear path-curvature response with respect to total velocity. Since the non-linear path-curvature responses decrease with increasing velocity, the automobile be understeered [11, 24]. The path curvature becomes a double-valved function because of the increased path curvature and decreased velocity which accompany large valuve of thrust. Hence, there can be two equilibrium conditions corresponding to a given path curvature and steer angle. For example, in the case of a 16-degree steer angle and a path curvature of 100 ft, equilibrium exists for velocities of approximately 46 and 51 ft/sec. The corresponding values of total thrust are 650 and 1010 lb, so that it is clear that large thrusts must be applied to reach the upper branches of the curves of path curvature response.

Figure 3.4 illustrates the non-linear path curvature response with respect to total input thrust. It can be seen that for large values of total thrust, the path curvatures reach a minimum and then increase.

Main factors that affect the tire side force are load transfer, driving thrust and slip angle. As the transferred load and driving thrust at the rear of the automobile increase, there is a sharp decrease in side force in the rear right tire. Therefore, to maintain a moment equilibrium a corresponding increase in side force of the rear left tire must be gen-

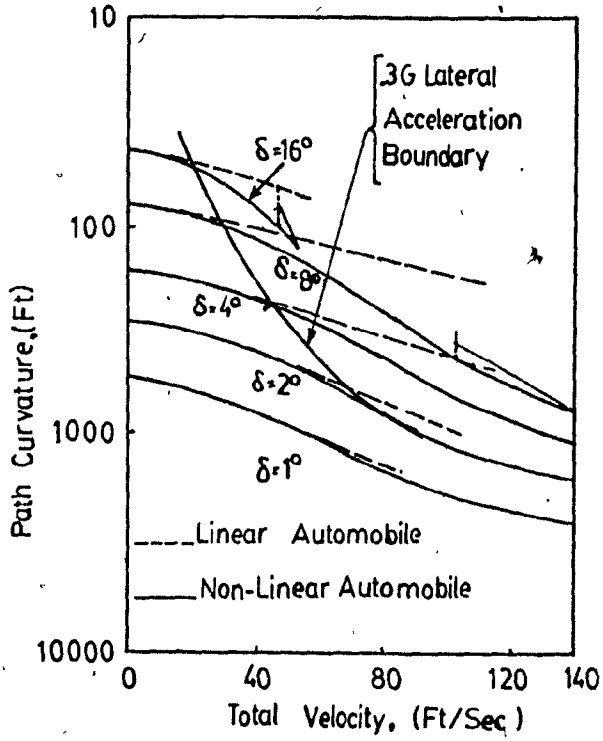

Fig. 3.3 - Path Curvature, 1/R Vs. Total Velocity, V

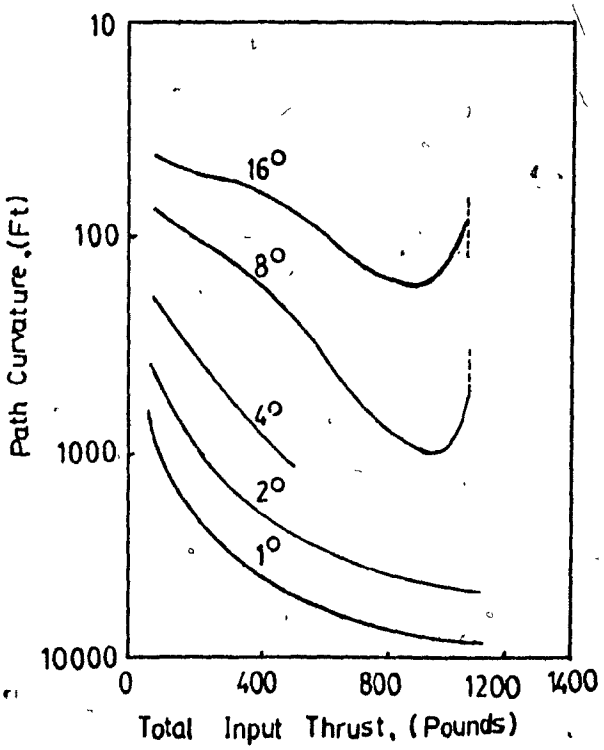

Fig. 3.4 Path Curvature, 1/R Vs. Total Input Thrust, P_{th}

erated. This increase of side force is produced by an increased slip angle at the rear relative to the front. Such an increase in the rear slip angle can be produced only by an increased yawing velocity.

Furthermore, the vehicle sideslip angle increases rapidly because of the need for both front and rear large slip angles, in order to maintain force equilibrium. As a result, the centrifugal force on the vehicle has a component, $(W n_y \sin \beta)$, which opposes the rear-wheel thrust. Hence, despite an increase of driving thrust, the velocity of the vehicle decreases.

This combination of increasing yawing velocity and decreasing vehicle velocity results in rapidly increasing path curvature since path curvature is equal to the ratio of yawing velocity to vehicle velocity.

The variation of path curvature with thrust, shown in Fig. 3.4, shows that as the driver gradually increases the throttle setting (the changes in throttle setting are assumed to be gradual so that equilibrium will exist at each combination of steer angle and thrust), holding the steer angle fixed, he will note a gradually decreasing path curvature and will appear to drift toward the outside of the curve. However, as he increases the thrust further, he will eventually pass the pont of minimum curvature and will then notice less of a tendency to drift to the outside of the curve. Furthermore, when he reaches large values of thrust, he will note an increased sensitivity of path curvature to changes in thrust, as indicated by the large positive slopes of the 8- and 16-degree curves of Fig. 3.4, for high thrust. This increased sensitivity to thrust is an example of the phenomena of 'steering by throttle', familiar to racing drivers.

It should be recognized that the above-mentioned changes in

path curvature with constant steer angle or changes in steer angle with constant steer angle or changes in steer angle with constant path-curvature are predicated on the assumption that sufficient torque is available from the engine to approach spinning of the inside rear wheel.

Figs. 3.5 and 3.6 illustrate the path curvature with steer angle for both constant velocity and thrust, respectively. As is demonstrated, the change of path curvature per unit change of steer angle decreases proportionally with increasing steer angle for constant velocity (Fig. 3.5). Inversely, there is an increase of the same, with increasing steer angle for constant thrust (Fig. 3.6).

Fig. 3.7 illustrates the lateral acceleration that is produced in a steady turn as a function of thrust for various constant steer angles. It is obvious that high lateral accelerations are produced by the larger steer angles and for high values of thrust. Interestingly enough lateral acceleration approaches an upper limit of approximately 0.75 at higher thrust values, irrespective of steer angle. Since the assumed coefficient of friction is unity, one might expect the maximum lateral acceleration to approach 1g. This high value of lateral acceleration is not achieved because the total horizonatal force produced by each of the rear tire is shared between side force and driving thrust, and the rear right wheel spin before all of the load is transferred from the inner (right) wheels to the outer (left) wheels. In practice, the effective maximum friction force between the tire and the road would most probably be less than the vertical load since the effect of the bouncing of the wheel affected by the degree of road roughness therefore, it cannot be expected to obtain measured lateral accelerations as high as 0.75.

Fig. 3.8 illustrates the load and total horizontal forces on

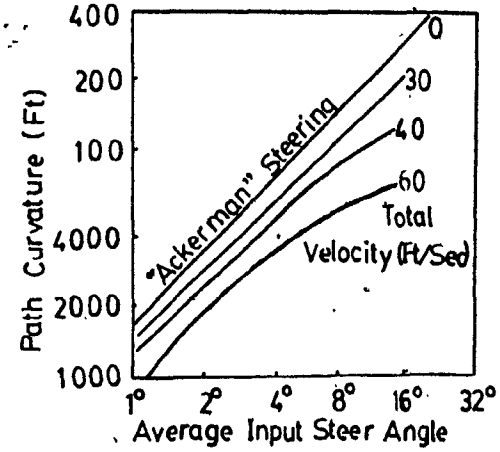

Fig. 3.5 - Path Curvature, 1/R, Vs. Steer Angle for Constant Velocity

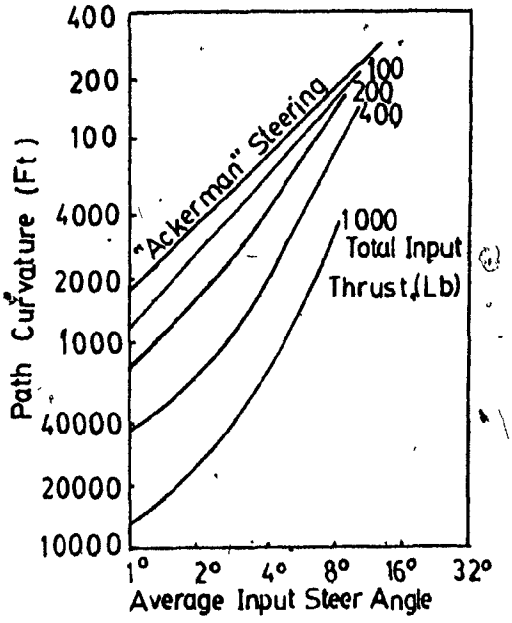

Fig. 3.6 - Path Curvature, 1/R, Vs. Steer Angle for Constant Thrust

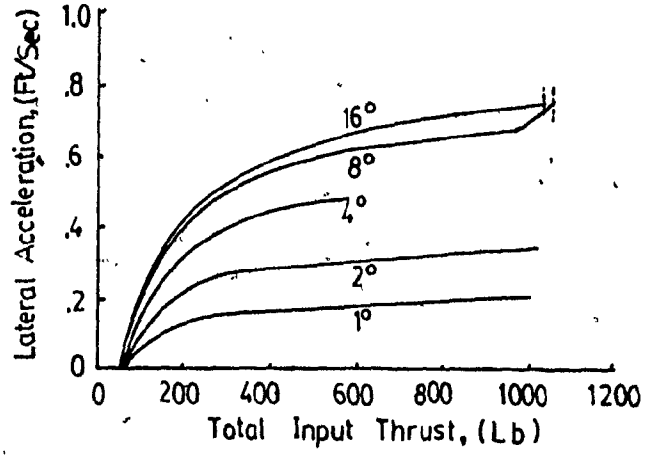

Fig. 3.7 - Lateral Acceleration, n_y Vs. Total Input Thrust, P_{th}

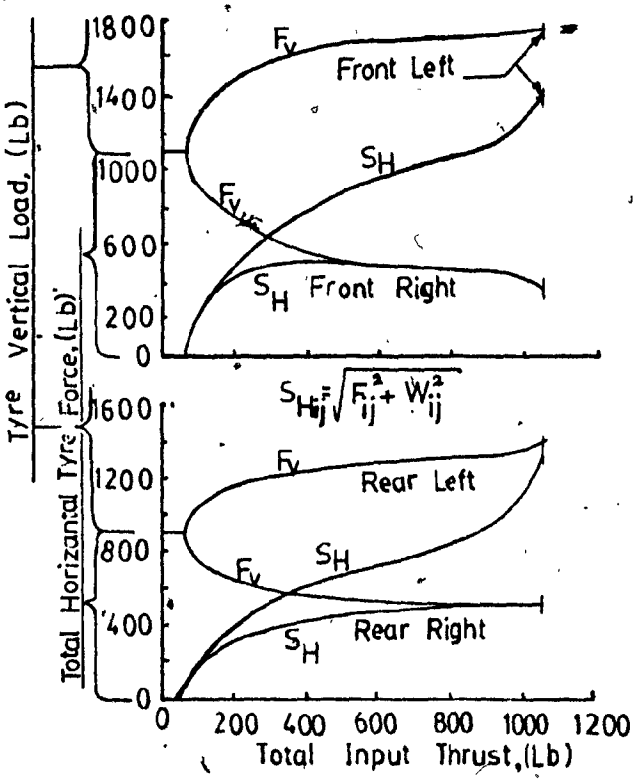

Fig. 3.8 - Tyre Vertical Load and Total Horizontal Tyre Force Vs. Total Input Thrust (δ=8 Degree)

each tire as a function of total thrust for an average steer angle of 8 degrees. It may be observed that the magnitude of the load transferred from one side of the automobile to the other varies in a manner similar to the curve for lateral acceleration versus thrust shown in Fig. 3.7. This similarity is expected because the moment due to the centrifugal force multiplied by the height of the centre of gravity above the ground is (approximately) balanced by the moment due to the differences in wheel load from side to side. In addition, it is seen that more load is transferred at the front than at the rear as a result of the greater front roll stiffness.

3.3 An Improved Model for Vehicle Dynamics

3.3.1 Derivation of Mathematical Model

The mathematical model described here was developed by E.A. Saibel and Shang-Lichang [13]. The model assumes a sprung mass mounted to the wheels by means of springs and dash pots. The springs and dash pots of the suspension system were assumed to be parallel and were connected with the wheel in series. Another pair of parallel non-linear tire springs and dashpots as shown in Fig. 3.9 were assumed to represent the visco-elastic behaviour of tires. A schematic equivalent of the vehicle for the transient analysis is shown in Fig. 3.10.

It is clear that by having the deflections of the springs, the motion of the sprung mass relative to the ground can be found. These are the Z_{ijk} where $i = 1.2$ and $j = L, R$ expresses rear right, right front, left front, and rear left, respectively. Road elevation, tire deflection, and spring deflection, are expressed by $k = 1, 2, 3$. It is assumed that yaw is unimportant than the roll angle ϕ and the motions of four wheel masses

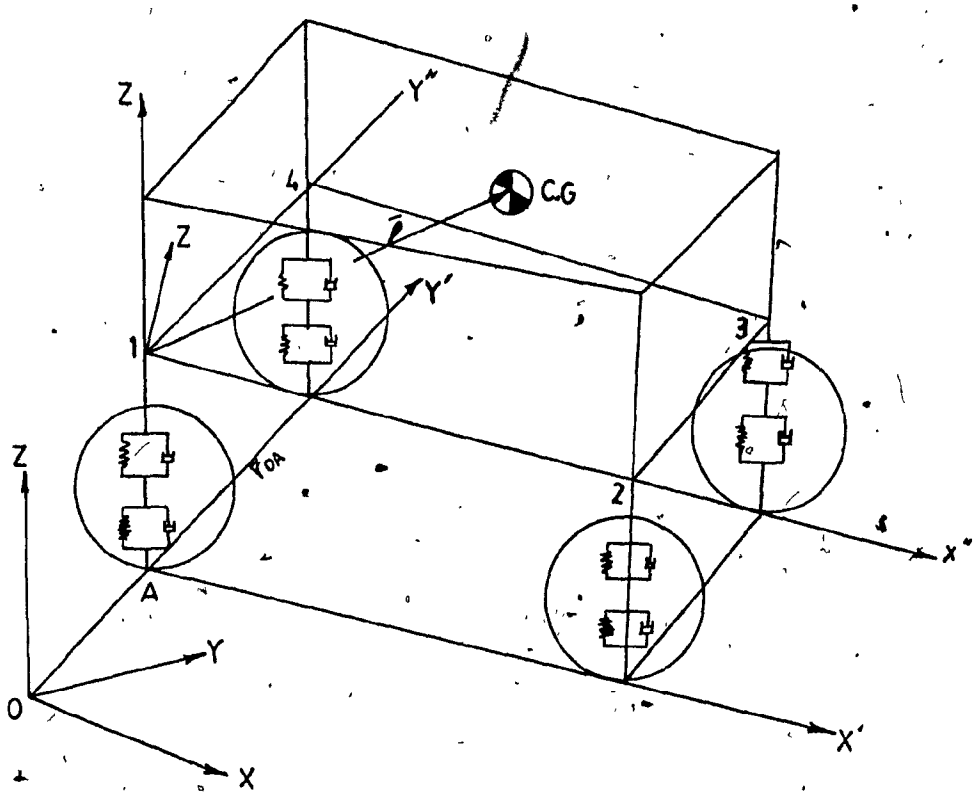

Fig. 3.9 - Coordinate System and Automobile

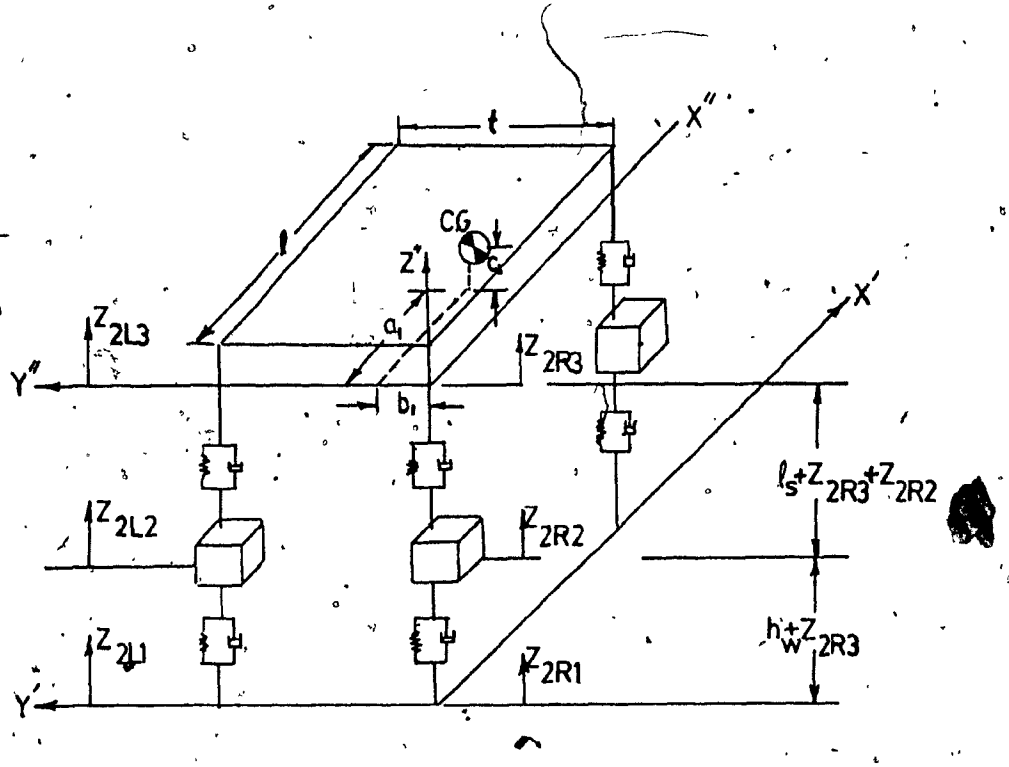

Fig. 3.10 - The Model Representing Road Elevation, Tyre Deflection and Spring Deflection

at points 1, 2, 3, 4 are vertical. Then the pitch angle Θ and the roll angle ϕ can be expressed as:

$$\phi = \frac{(Z_{2L3}) - (Z_{2R3})}{t} = \frac{(Z_{1L3}) - (Z_{1R3})}{t} \quad \ldots\ldots\ldots\ldots (3.26)$$

$$\Theta = \frac{(Z_{2R3}) - (Z_{1R3})}{l} = \frac{(Z_{2L3}) - (Z_{1L3})}{\ell} \quad \ldots\ldots\ldots\ldots (3.27)$$

In order to find the acceleration of the centre of gravity, the following kinematic relationship can be written:

$$\ddot{\vec{r}} = \ddot{\vec{R}} + \ddot{\vec{\rho}}_{rel} + 2\,\vec{\omega} \times \dot{\vec{\rho}}_{rel} + \dot{\vec{\omega}} \times \vec{\rho} + \vec{\omega} \times (\vec{\omega} \times \vec{\rho}) \quad \ldots\ldots\ldots\ldots (3.28)$$

Since a three-coordinate system is used, the acceleration of the center of gravity relative to point O in Fig. 3.9 will be obtained by first finding the acceleration of the center of gravity relative to point A. Using equation (3.28), and Fig. 3.11,

$$\ddot{\vec{r}}_A = \ddot{Z}_{2R3}\vec{k}'' + c\ddot{\Theta}\,\vec{i}'' - c\dot{\phi}\dot{\Theta}\,\vec{j}'' + (b\ddot{\phi} - a\ddot{\Theta})\vec{k}'' + (b\dot{\phi}\dot{\Theta} - a\dot{\Theta}^2)\,\vec{i}''$$
$$- (b\dot{\phi}^2 - a\dot{\phi}\dot{\Theta})\,\vec{j}'' - (c\dot{\phi}^2 + c\dot{\Theta}^2)\vec{k}'' \quad \ldots\ldots\ldots\ldots (3.29)$$

This equation expresses the acceleration of the center of gravity relative to point A. In order to find the acceleration of the center of gravity relative to the inertial frame, apply equation (3.28) again to the system shown on Fig. (3.12). In this system, $\ddot{\vec{\rho}}_{rel}$ has the physical meaning of the acceleration of the center of gravity relative to A, which is equal to $\ddot{\vec{r}}_A$ shown on equation (3.29).

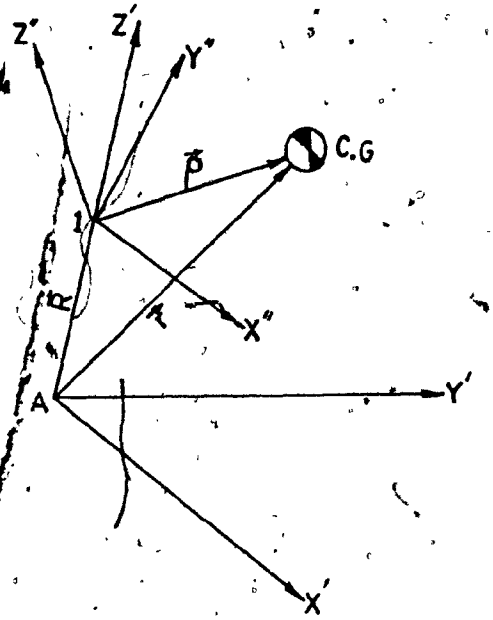

Fig. 3.11 - The Position Vectors of C.G. Relative to Point A

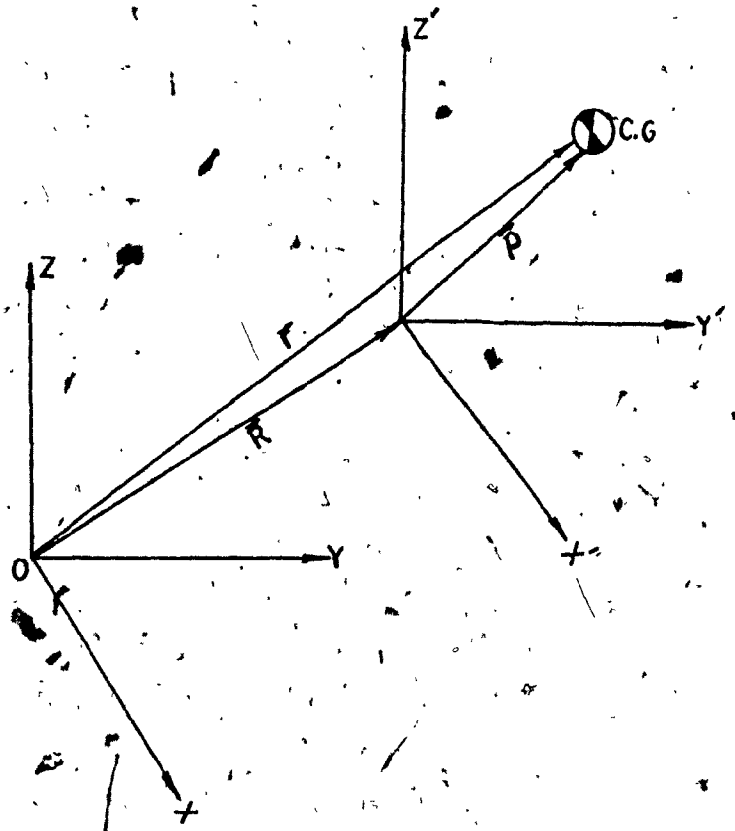

Fig. 3.12 - The Position of C.G. Relative to a Fixed System and Moving System

Also ϕ and θ are small quantities and hence ϕ^2, θ^2, and $\dot{\phi}\dot{\theta}$, can be neglected compared with $\ddot{\phi}$, $\ddot{\theta}$, and $\ddot{Z}_{13}$ terms. After finding $\vec{\rho}_{rel}$, $\vec{R}$ and transforming the double prime system to a single prime system and substituting these quantities into equation (3.28):

$$\vec{r} = c\ddot{\theta}\,\vec{i}' - c\ddot{\phi}\,\vec{j}' + (\ddot{Z}_{2R3} + b\ddot{\phi} - a\ddot{\theta})\vec{K}' + \ddot{x}_1\vec{i} + \ddot{y}_1\vec{j} \quad \ldots\ldots (3.30)$$

In the study of vehicles along a straight line, we know $i = i'$, $j = j'$. Because the vehicles are constrained to go along a straight line, we will assume vehicles have no roll angle. Hence equation (3.30) reduces to

$$\vec{r} = (\ddot{x}_1 + c\ddot{\theta})\vec{i}' + (\ddot{Z}_{2R3} - a\ddot{\theta})\vec{k}' \quad \ldots\ldots\ldots (3.31)$$

The moment of the external forces about the C.G. is given by

$$\vec{G}_G = \vec{h}_G \quad \ldots\ldots\ldots\ldots\ldots\ldots (3.32)$$

where

$$\vec{h}_G = h_{xc}"\vec{i}" + h_{yc}"\vec{j} \;\; P \;\; h_{zc}"\vec{k}"$$

$$h_{xc}" = I_x\omega_{x}" - I_{xy}\omega_{y}" - I_{xz}\omega_{z}"$$

$$h_{yc}" = I_{xy}\omega_{x}" + I_{yy}\omega_{y}" - I_{yz}\omega_{z}"$$

$$h_{zc}" = -I_{xz}\omega_{x}" - I_{yz}\omega_{z}" + I_z\omega_z$$

The $\omega_x"$, $\omega_y"$ and $\omega_z"$ are the absolute angular velocities of the double prime system, and $h_{xc}"$, $h_{yc}"$ and $h_{zc}"$ are moment of momentum relative to origin frame at C.G.

For convenience, axes passing through the center of gravity, parallel to the double prime system, and fixed in the body, (i.e. X_c", Y_c", Z_c"). Because of symmetry, $I_{xy} = I_{yz} = 0$.

The absolute angular velocity of the double prime is:

$$\omega_{abs} = \dot{\phi}\vec{j}" + \dot{\theta}\vec{j}"$$

$$= \omega_{x"}\vec{i}" + \omega_{y"}\vec{j}" + \omega_{z"}k" \quad \ldots\ldots\ldots\ldots\ldots (3.33)$$

Substituting equation (3.33) into equation (3.32) gives —

$$\vec{h}_G = I_x \dot{\phi}\vec{i}" + I_y \dot{\theta}\vec{j}" - I_{xz}\dot{\phi}\vec{k}"$$

$$\dot{\vec{h}}_G = I_x \ddot{\phi}\vec{i}" + I_y \ddot{\theta}\vec{j}" - I_{xz}\ddot{\phi}\vec{k}" + I_x\dot{\phi}\dot{\vec{i}}" + I_y\dot{\theta}\dot{\vec{j}}" - I_{xz}\dot{\phi}\dot{\vec{k}}"$$

By converting from the double prime to the single prime system and ignoring higher order terms, the following equation is obtained:

$$\dot{\vec{h}}_G = I_x\ddot{\phi}\vec{i}' + I_y\ddot{\theta}\vec{j}' - I_{xz}\ddot{\phi}\vec{k}'$$

For vehicle along a straight line (no roll angle)

$$\dot{\vec{h}}_G = I_y \ddot{\theta}\vec{j}' \quad \ldots\ldots\ldots\ldots\ldots\ldots\ldots (3.34)$$

In order to write the equation of motion, $\vec{G}_G = \dot{\vec{H}}_G$ and $\vec{F} = \vec{ma}$ has been used. Let S_{ij} ($i = 1, 2$ and $j = L, R$) express the effective tractive effort. Since S_{ij} not only accelerate the wheel, but also transfers part of it to accelerate the sprung mass, we can obtain the following:

$$S_{ij_s} = S_{ij} - \frac{W_w}{g}\ddot{x}_{ij} \quad \ldots\ldots\ldots\ldots\ldots (3.35)$$

moment couples will be introduced if forces are shifted from one location to another. Therefore, the moment couples in y' direction are:

$$N_{ijy'} = -(\ell_s + Z_{ij3} - Z_{ij2})S_{ij_s} - (h_w + Z_{ij2})S_{ij} \quad \ldots \quad (3.36)$$

Now define a dynamic wheel load as the instantaneous value of vertical reaction between the tire and the road surface and assume that the engine power is equally divided in the wheels, or that brake forces are equally distributed. In addition for vehicles travelling on a straight path, the lateral forces are balanced out. Hence, $S_{2R} = S_{2L}$, $S_{1R} = S_{1L}$, $Z_{2R2} = Z_{2L2}$, $Z_{2R3} = Z_{2L3}$, $Z_{1R2} = Z_{1L2}$, and $Z_{1L3} = Z_{1R3}$. Therefore, the equations of motion can be written as follows:

$$2S_{2R} + 2S_{1R} - 4\frac{W_w}{g}\ddot{x} - \text{wind force} = (\ddot{x} + c\ddot{\theta})\frac{W_s}{g} \quad \ldots \quad (3.37)$$

$$2k_s(Z_{2R2} - Z_{2R3}) + 2k_s(Z_{1R2} - Z_{1R3}) + 2C_s(\dot{Z}_{2R2} - \dot{Z}_{2R3}) + 2C_s(\dot{Z}_{1R2} - \dot{Z}_{1R3})$$
$$= (\ddot{Z}_{2R3} - a\ddot{\theta})\frac{W_s}{g} \quad \ldots \quad (3.38)$$

$$2k_s a(Z_{2R2} - Z_{2R3}) + 2C_s a(\dot{Z}_{2R2} - \dot{Z}_{2R3}) - 2k_s(1-a)(Z_{1R2} - Z_{1R3})$$
$$-2C_s(1-a)(\dot{Z}_{1R2} - \dot{Z}_{1R3}) + \text{e. wind} + (S_{2R_s} + S_{1R_s})(a\theta - c)$$
$$-S_{1RS}\ell\theta + 2\frac{W_w}{g}(2\ell_s + Z_{2R3} + Z_{1R3} - Z_{2R2} - Z_{1R2})\ddot{x}$$
$$-2(\ell_s + h_w + Z_{2R3})S_{2R} - 2(\ell_s + h_w + Z_{1R3})S_{1R} = I_y\ddot{\theta} \quad \ldots \quad (3.39)$$

$$\theta = (Z_{2R3} - Z_{1R3})/\ell \quad \ldots \quad (3.40)$$

$$\frac{W_w}{g}\ddot{Z}_{2R2} + K_t Z_{2R2}^{1.76} + C_t\dot{Z}_{2R2} + K_s(Z_{2R2} - Z_{2R3}) + C_s(\dot{Z}_{2R2} - \dot{Z}_{2R3}) = 0 \quad \ldots\ldots\ldots (3.41)$$

$$\frac{W_w}{g}\ddot{Z}_{1R2} + K_t Z_{1R2}^{1.76} + C_t\dot{Z}_{1R2} + K_s(Z_{1R2} - Z_{1R3}) + C_s(\dot{Z}_{1R2} - \dot{Z}_{1R3}) = 0 \quad \ldots\ldots\ldots (3.42)$$

where Eq. 3.37 and 3.42 are the equations of motion of the wheel, $z^{1.76}$ expresses the non-linear tire characteristics., Radt and Pacejka [26] have arrived at empirical formulas which can be used in expressing such factors as the rolling resistance and wind forces.

Rolling resistance = $F_v(A' + B'v)$

Wind force $X_w = 1/2\ C_w A_r \nu \dot{x} |\dot{x}|$

where

C_w = 0.45, coefficient of wind

A_r = the area of automobile in the largest section, ft^2

F_v = the vertical load on each tire, lb_f

$\dot{X}$ = the velocity of the car, ft/sec.

The set of equation (3.37) to (3.42) completely describe the dynamic behaviour of vehicles during braking.

3.2.2 Results and Discussion

Sabile and Shang [13] have studied the dynamic behaviour of a vehicle during braking based on the above set of equations. Fig. 3.13 shows the comparison between front, rear, four wheel and cross wheel braking,

where S_{2R} = 600 lb_f on each rear wheel or front wheel brake, S_{1R} = 300 lb_f on each wheel brake and S = 600 lb_f for either right front, left rear, or right rear, left front cross braking and initial velocity of the vehicle before braking is taken to be 60 MPH are taken.

All the physical properties of the vehicle are shown in Table 3.1. Fig. 3.14 shows the change in normal force when steel spring constant (k_s) are different. Fig. 3.13 is the comparison of the effect of vertical forces exerted on the car by individually testing the effects of four different types of brakes, i.e. 1. rear wheel brake 2. front wheel brake 3. four wheel brake 4. cross brake.

It is obvious that in the aforementioned four cases, the motion of the braking duration is damped oscillatory. However, the figure shows that the four wheel brake-type is preferable since it reaches the steady state response sooner than the others, therefore it requires less vertical force and minimizes the body tremor.

Fig. 3.14 indicates that under the same normal force, higher the k_s, higher the frequency of oscillation. Consequently, lower the k_s, lower the frequency. Therefore, it is more advantageous to select the spring with lower k_s.

3.4 Calculation of Lateral Tire Forces

A number of tire tests performed at slow speed on a plane dry concrete surface have been used to synthetize a typical general curve which can be used in the vehicle response calculations. Referring to the diagram, Fig. 3.15, the braking (tire) forces S are obtained by braking or accelerating the wheel, L is the lateral force which is obtained when

Table 3.1 -- Parameters of Automobile and Type.

l	=	119/12 ft.
a	=	(5.5/9.9)1 ft.
b	=	(1/2)1 ft.
c	=	(1/2)1 ft.
t	=	(62/12) ft.
K_t	=	19,00 $[F=K_tZ^{1.76}]$
C_t	=	48 3200 lb_f - sec. ft.
$I_{xc"}$	=	540 lb-ft-sec .
$I_{yc"}$	=	3.350 lb-ft-sec
$I_{xc"Z"c}$	=	260 lb-ft-sec .
E_s	=	0.4 ft.
C_s	=	150 lb_f-sec/ft
K_s	=	108 lb_f/in
W_s	=	4,500 lb
W_w	=	40 lb
S_{2R}	=	600 lb_f.
S_{1R}	=	300 lb_f.
S	=	600 lb_f.

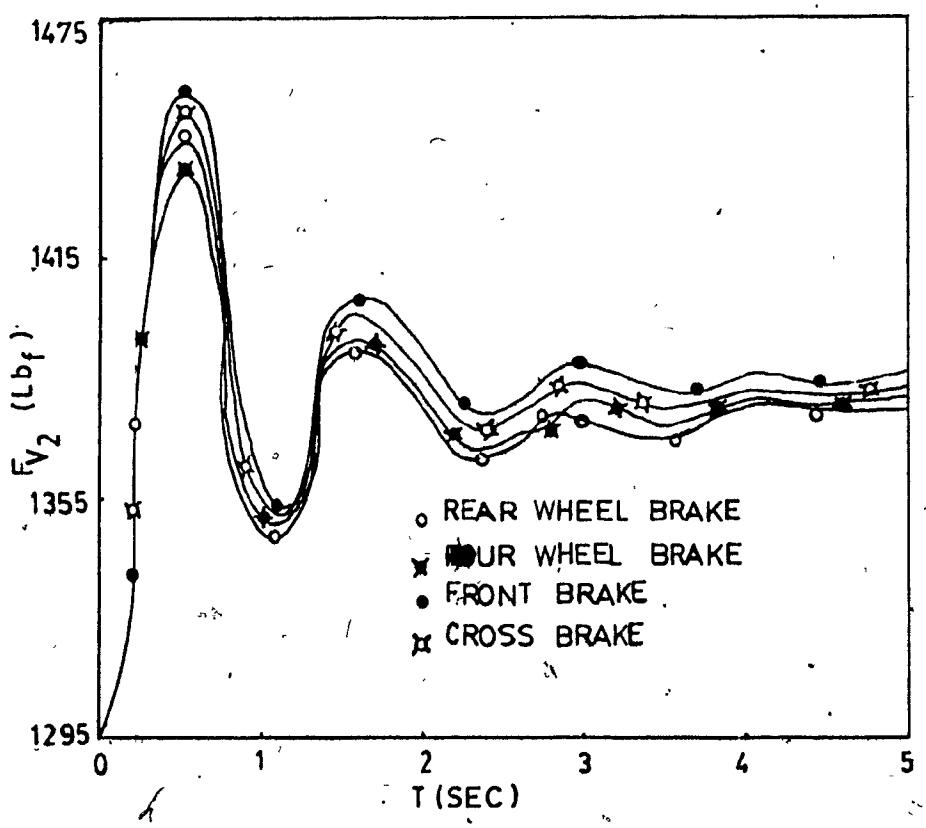

Fig. 3.13 - Vertical Forces Vs. Time

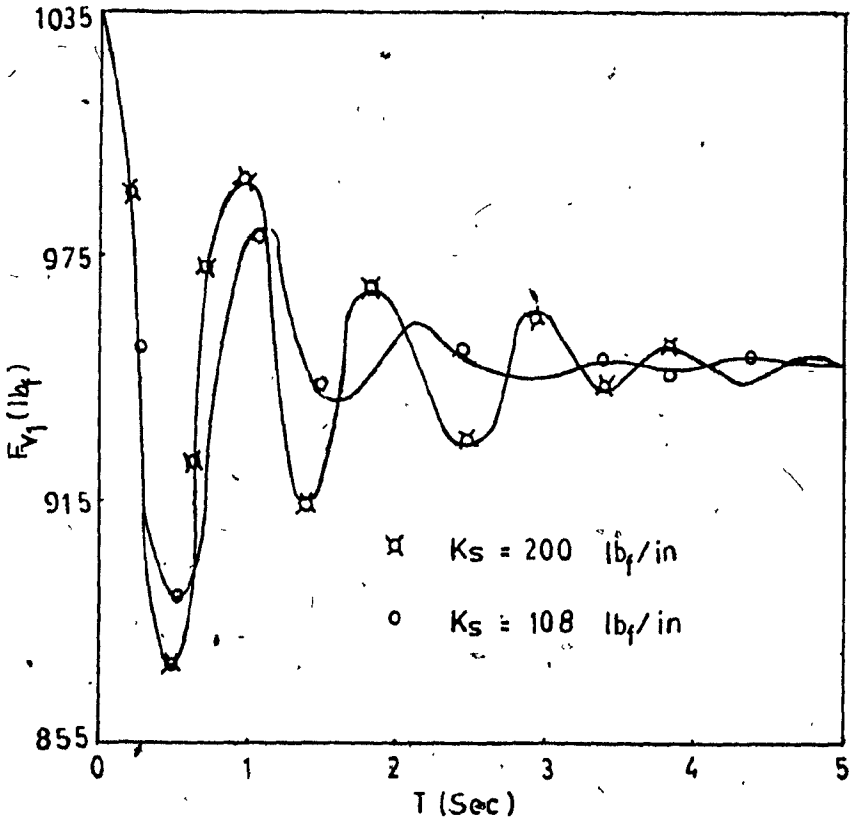

Fig. 3.14 - [illegible]orce Under Wheel 1 Vs. Time, Brake

the tire is side slipping at an angle χ while under the action of a force S.

Fig. 3.16 shows that the increase in the lateral force with an increase in the side slip angle and it can be seen that the lateral force, L, reaches a maximum value at 12^0 sideslip angle, when the tire has no fore and aft forces. When afore and aft force is applied, it reduces the maximum lateral force which may be developed. Fig. 3.17 represents the maximum ground to tyre force which can occur before an "all sliding" state is reached. If braking force S is applied the maximum lateral force is:

$$L = \sqrt{(\mu_A W)^2 - S^2}$$

Several theories of the lateral distortion of a tire during steering are available. Temple and von Schlippe [26], considered the tire as a tensioned string on a continuous elastic support. Filla [27] and Bergman [19] based their analyses upon the beam on elastic foundation theory and presented semi-empirical analyses from which cornering force coefficients are calculated. Thorson [20] considered the beam with tension on an elastic support. All these theories rely to some extent on measured tire data, and it is not possible to predict cornering force coefficients from a purely theoretical basis.

3.5 "Pulsed" Braking [28]

"Sensing units" sense angular acceleration at the wheels of a vehicle. These units monitor the hydraulic supply line pressure which results in the application of braking force as a series of pulses. If the braking force is thus applied, then the lateral forces will also appear

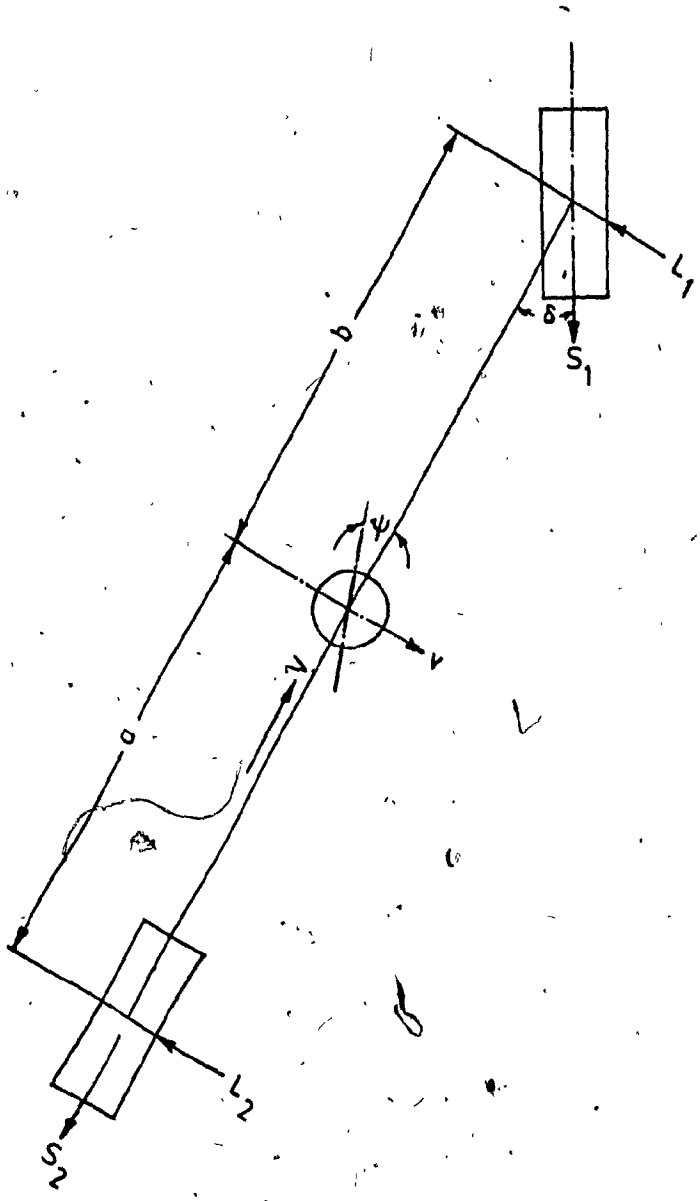

Fig. 3.15 - Symbols and Forces Used in the Representation of the Passenger Car

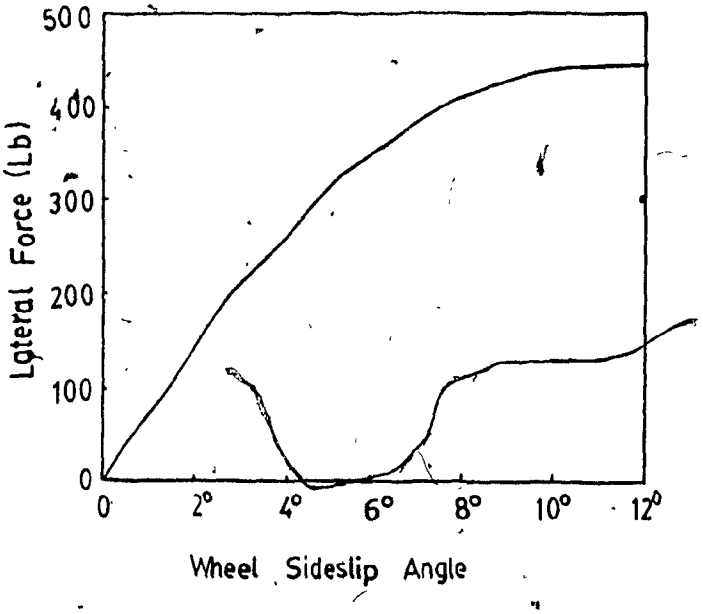

Fig. 3.16 - The Positive Branch of the Tyre Lateral Force Vs. Side Slip Angle Curve

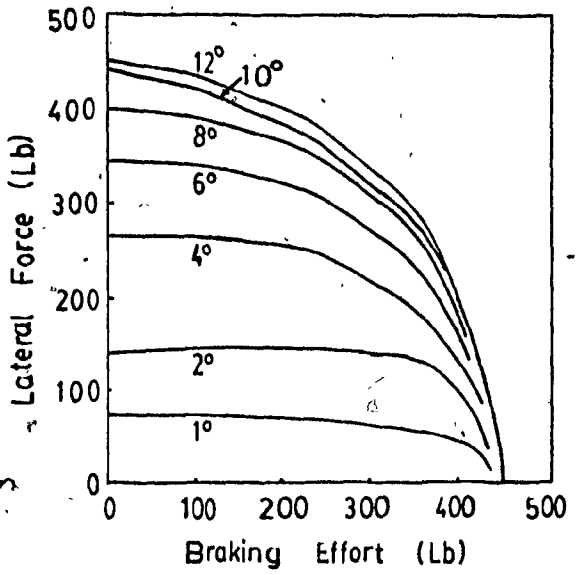

Fig. 3.17 - The Assumed Effects of Braking on the Lateral Force Produced at Constant Side Slip Angles